The rainbow instanton method: A new approach to tunneling splitting in polyatomics

Zorka Smedarchina, Willem Siebrand, and Antonio Fernández-Ramos

Citation: J. Chem. Phys. **137**, 224105 (2012); doi: 10.1063/1.4769198
View online: http://dx.doi.org/10.1063/1.4769198
View Table of Contents: http://jcp.aip.org/resource/1/JCPSA6/v137/i22
Published by the American Institute of Physics.

The rainbow instanton method: A new approach to tunneling splitting in polyatomics

Zorka Smedarchina,[1] Willem Siebrand,[1] and Antonio Fernández-Ramos[2]
[1]*National Research Council of Canada, Ottawa, Ontario K1A 0R6, Canada*
[2]*Department of Physical Chemistry and Centro Singular de Investigación en Química Biolóxica e Materiales Moleculares (CIQUS), University of Santiago de Compostela, 15782 Santiago de Compostela, Spain*

(Received 25 July 2012; accepted 14 November 2012; published online 11 December 2012)

A new instanton approach is reported to tunneling at zero-temperature in multidimensional (MD) systems in which a "light particle" is transferred between two equivalent "heavy" sites. The method is based on two concepts. The first is that an adequate MD potential energy surface can be generated from input of the stationary configurations only, by choosing as a basis the normal modes of the transition state. It takes the form of a double-minimum potential along the mode with imaginary frequency and coupling terms to the remaining (harmonic) oscillators. Standard integrating out of the oscillators gives rise to an effective 1D instanton problem for the adiabatic potential, but requires evaluation of a nonlocal term in the Euclidean action, governed by exponential (memory) kernels. The second concept is that this nonlocal action can be treated as a "perturbation," for which a new approximate instanton solution is derived, termed the "rainbow" solution. Key to the approach is avoidance of approximations to the exponential kernels, which is made possible by a remarkable conversion property of the rainbow solution. This leads to a new approximation scheme for direct evaluation of the Euclidean action, which avoids the time-consuming search of the exact instanton trajectory. This "rainbow approximation" can handle coupling to modes that cover a wide range of frequencies and bridge the gap between the adiabatic and sudden approximations. It suffers far fewer restrictions than these conventional approximations and is proving particularly effective for systems with strong coupling, such as proton transfer in hydrogen bonds. Comparison with the known exact instanton action in two-dimensional models and application to zero-level tunneling splittings in two isotopomers of malonaldehyde are presented to show the accuracy and efficiency of the approach. [http://dx.doi.org/10.1063/1.4769198]

I. INTRODUCTION

Dynamic properties of quantum systems are often expressed in terms of particles tunneling through a barrier. One of the theoretical approaches to such problems, and the one used in this article, is the instanton approach, in which tunneling in a multidimensional (MD) configuration space is described as 1D motion along a unique path, the instanton, where the tunneling probability is maximal.[1] Because of its efficiency, this method has recently found application to many tunneling problems in chemistry and even biology.[2] The purpose of this article is to introduce a new approach to tunneling at zero-temperature in MD systems where a "light particle" is transferred between two equivalent "heavy" sites. The approach proposed here differs from other approaches, including our earlier approximate instanton method (AIM),[3] and promises good accuracy obtained with minimal computational effort. Although the new method is general, for definiteness we concentrate on zero-level tunneling splitting caused by proton tunneling along hydrogen bonds in molecules and complexes. This example has the benefit of allowing comparison with observed splittings and is sufficiently complex to show the merits of the method relative to other available methods.

The first application of instanton technics to problems of this type was carried out in a pioneering study by Makri and Miller,[4] where the authors assume that tunneling is "fast" relative to the other motions and takes place in an effective 1D potential along a "straight" path between turning points. In the alternative case, the "slow" tunneling takes place in an effective 1D potential along the minimal energy path.[5] These approximations, referred to as the "fast-flip" or sudden approximation (SA), and the "slow-flip" or adiabatic approximation (AA), respectively, are reviewed in the book by Benderskii, Makarov, and Wight.[1] Much of the recent progress in the field is due to the group of Benderskii,[1,6] which found instanton solutions for a variety of low-dimensional models with a double-minimum potential coupled to other degrees of freedom. Although these methods can produce accurate solutions for simple systems, the results are not readily generalized to MD systems, where tunneling is coupled to many degrees of freedom with a complex spectrum and of different symmetry. To deal with such systems, we return to the basic definitions of the instanton approach, relating the tunneling probability to the imaginary part of the partition function, which can be calculated as the trace of the density matrix.[1] Using the relation of the density matrix to the time-evolution operator, the partition function is expressed as a sum over all possible paths $s(t)$ in configuration space (a path integral), each contributing with the phase factor $\exp(iS)$, where S is the classical action (hereafter action is in units $\hbar$). The resulting oscillatory behavior is overcome by transformation

to imaginary time $t \rightarrow \tau = it$, each path acquiring the "weight" $\exp(-S_E)$, where $S_E = \int d\tau\, H[s(\tau)]$ is the Euclidean action, defined via the Hamiltonian $H = \frac{1}{2}\dot{s}^2 + V(s)$, instead of the Lagrangean; it describes classical motion in the upside-down potential $V(s) \rightarrow -V(s)$. The path where the tunneling probability reaches its maximum value, i.e., where S_E has a minimum, is called the instanton; we denote it by s_I. The tunneling probability is then defined by a single term: $P \sim \exp(-S_E)$, where $S_E = \int d\tau\, [\frac{1}{2}\dot{s}_I^2 + V(s_I)]$ is the Euclidean action evaluated along the extreme path, called hereafter instanton action.

Application of this elegant idea to MD systems is not a trivial task, mainly because the result is very sensitive to the accuracy of the instanton action S_E which enters as an exponent. The common approach, pursued by Tautermann *et al.*;[7] Meana-Paña *et al.*;[8] Mil'nikov and Nakamura;[9] and, more recently, Richardson *et al.*;[10] and Rommel and Kästner,[11] involves a search for the instanton trajectory via direct minimization of the Euclidean action, and then evaluating it along this path. Thus the MD potential (and the Euclidean action) is generated on a grid in the configuration space of $3N - 6$ dimensions, N being the number of atoms, until the trajectory is found where the action reaches its minimal value. This approach requires, on the one hand, a sufficiently dense grid, and on the other, accurate evaluation of the MD potential in each point. Although the method is easy to apply, since it involves frequently repeating the same routine computation, its cost may be prohibitive unless the level of computation or the density of the grid is taken lower than optimal. The method has been applied to a variety of proton tunneling processes in molecules and complexes, with mixed results, as discussed in Sec. VI. Since the instanton path is not the same for different isotopomers, extension to deuterium tunneling, for instance, requires repeating the entire calculation; the procedure may be abbreviated by mass-scaling of the grid, but this will affect the accuracy.

We adopted an alternative approach by making an educated guess of the instanton on physical grounds, and generating the MD potential based on symmetry; to our knowledge this was the first full-dimensional instanton application to real systems reported in the literature.[12] We took advantage of the symmetry with respect to reflection in the dividing plane, say $x = 0$, by recognizing that the instanton, in the vicinity of the plane, must coincide with the direction x perpendicular to it. We thus adopted x as the "reaction coordinate" and constructed the MD potential as a sum of a (symmetric) double-minimum potential $V(x)$ that connects the minima and coupling terms to the remaining $3N - 7$ degrees of freedom $\{y\}$ perpendicular to x. As a basis set we employed the (mass-weighted) normal modes (x, $\{y\}$) of the transition state (TS) configuration, which is the configuration of highest symmetry, x being the mode with imaginary frequency. This choice allowed direct generation of the MD potential in the multi-term form $V(x) + \omega_i^2 y_i^2/2 + C_i x^n y_i^m$, where $V(x)$ and the constants $\{C\}$ of the leading coupling terms allowed by symmetry are evaluated from standard electronic-structure and force field data for two stationary configurations only: the equilibrium configuration (EQ) and the TS. In solving the instanton problem for this potential, our earlier AIM (Ref. 3) made use of the instanton action derived by Benderskii *et al.* for model systems.[6] We introduced simplifications that allowed generalization of these results to MD systems, where some of the coupled modes are "fast," some "slow" on the time scale of tunneling. This approach allowed us to derive rates and splittings directly from the instanton action, thereby circumventing the large number of structural calculations required to determine the exact instanton trajectory. Computationally the method, as implemented in the DOIT program[3] is not demanding and has been applied to proton tunneling in a wide variety of molecules and complexes.[2,3,12,13] It has also been successfully generalized to splittings of vibrationally excited levels. For instance, it predicted correctly,[14] in contradiction to the proposal of the original authors[15] and some earlier estimates,[16] that in the formic acid dimer, which represents a well-known test case for tunneling splittings, the splitting of the zero-point level exceeds that of an excited CO-stretch level.[17] Nevertheless, because of the approximations involved, problems are encountered, as shown below, especially when the coupling is strong.

Subsequently Benderskii *et al.*[18] developed a perturbative instanton approach (PIA), both for ground and excited state splittings, using a generalization to the AIM Hamiltonian. However, this method remains to be tested for the systems of interest in the present study; whether it can deal with systems in which the coupling is strong remains to be established.

Since the results of our method are comparable to those of the other methods cited above, its simplicity would make it the method of choice if the strong coupling problem can be solved. In the AIM approach, this problem arises because the approximations developed for the nonlocal part of the Euclidean action depend on the relation of the frequency of the coupled modes to the time scale of tunneling. To make use the results of Benderskii for 2D systems,[6] high-frequency ("fast") modes are treated in the AA, and low-frequency ("slow") modes in the SA, which formally means replacing the exponential kernels in the non-local action by delta-functions, and by their expansion over small parameters, respectively.[1,19] Their effect on tunneling is different, fast modes leading to renormalization of the mass of the tunneling particle and slow modes leading to barrier modulations. This different behavior becomes critical in the intermediate region where the effect may go both ways. This may give rise to ambiguous results or, at least, to results that are extremely sensitive to the quality of the calculated potential. This ambiguity arises in systems with strong hydrogen bonds where a high hydrogen-bond frequency is strongly coupled to the proton motion. Such strongly coupled motions are not adequately described by approximation schemes for the kernels appearing in the AA or SA.

In the present contribution we address this problem by a two-step instanton approach. First we represent the Euclidean action as a sum of a local and nonlocal parts, where the latter remains relatively small even in the case of strong coupling and can be treated as a "perturbation". Keeping the exponential kernels intact, we then evaluate the nonlocal part based on a suitable approximate instanton solution, termed rainbow solution, which we derive. As a result, the instanton

action is now represented as a sum of two terms, a main term representing the instanton action of a 1D motion in the adiabatic potential, and a correction term thus evaluated. This approach allows us to deal conveniently with strong coupling, because the reduced imaginary frequency tends to move the most strongly coupled mode(s) towards the "fast" group; an adequate approximate solution can thus be obtained by treating these most important modes in the AA; the remaining (weakly coupled) modes can be treated in the AA or in the SA, based on the implied separation criterion. We refer to this approach as the rainbow approximation because of its ability to handle a wide range of vibrational frequencies that bridge the gap between the limits where the AA and SA apply. We note that the method retains the main advantage of the AIM approach, namely the circumvention of the large number of structural calculations required to determine the exact instanton trajectory.

In Sec. II, we give a general outline of this method and present the results in a form that is convenient for practical applications. In Sec. III, we provide a detailed derivation to justify these results; this section may be skipped on first reading by readers primarily interested in practical tests. In Sec. IV, we define the zero-level tunneling splitting within the rainbow approach. In Sec. V, the performance of the method is formally tested for a 2D model for which exact instanton solutions are known, namely tunneling in a quartic potential coupled symmetrically to a single harmonic mode. This test is used to find out whether the approach is basically sound. The ultimate test will be a comparison with realistic systems. For this purpose we choose in Sec. VI the molecule malonaldehyde of which the observed splittings for proton and deuteron tunneling are widely used as a benchmark for calculations of such splittings. Other, more complex systems we have examined are briefly mentioned; they will be discussed in detail in a subsequent article, hereafter referred to as Part II.

II. GENERAL OUTLINE

A. The Hamiltonian

We consider tunneling at zero temperature of a particle of unit mass in a symmetric 1D double-well potential $V_{1D}(Q)$ coupled to a system of harmonic oscillators $\{q, \omega\}$ through couplings linear in $\{q\}$. The Hamiltonian is similar to that previously derived and applied in AIM.[3] Its generation from quantum-chemical calculations is summarized in the Appendix; a more detailed account can be found in Ref. 3. In dimensionless units it takes the general form

$$H = \frac{1}{2}\dot{Q}^2 + \frac{1}{2}\sum_i \dot{q}_i^2 + V(Q,\{q\}),$$
$$V(Q,\{q\}) = V_{1D}(Q) + \sum_i \gamma_i \Lambda_i(Q) q_i + \frac{1}{2}\sum_i \omega_i^2 q_i^2, \quad (1)$$

where $V_{1D}(Q)$ has a maximum (=1) at $Q = 0$ and minima (=0) at $|Q| = 1$. Since the system is symmetric under reflection in the dividing plane $Q = 0$, the coupled oscillators in Eq. (1) can be divided into groups of symmetric modes $\{q_s\}$ and of antisymmetric modes $\{q_a\}$. The leading coupling terms allowed by symmetry are then of the type Qq_a and Q^2q_s, i.e., correspond to $\Lambda_{(a)}(Q) \sim Q$, $\Lambda_{(s)}(Q) \sim Q^2$ in Eq. (1). Here and hereafter, we use subscripts s and a as labels and subscript i as a running number. The coupling constants γ_i are proportional to the displacements of the modes q_i between the TS and EQ; undisplaced modes do not contribute: $\Lambda_{i\neq a,s}(Q) = 0$. Higher-order (weaker) coupling terms of the type Q^2q^2, etc., are not included in this Hamiltonian explicitly, but are effectively accounted for by a recalibration of the constants γ_i of linear coupling. This recalibration is done in such a way that the most important parameter, namely the adiabatic barrier height, to be obtained from Eq. (1), is identical with the barrier height obtained quantum-chemically for the *real* potential energy surface (PES). Kinematic couplings are neglected throughout, and so are couplings between the oscillators of the type q_iq_j, etc. We address the adequacy of this Hamiltonian to real systems at the end of this subsection.

As defined in the Introduction, in our approach we use the set $(x, \{y\})$ of (mass-weighted) normal modes of the TS configuration, the mode x with imaginary frequency serving as the "reaction coordinate." The parameters are generated from electronic structure and force field calculations for the EQ and the TS configurations. $V_{1D}(x)$ is generated as the potential with the coupled oscillators $\{y\}$ frozen in their equilibrium positions; it is equivalent to the potential along the linear reaction path (LRP). Its height V_0 and (mass-weighted) halfwidth Δx are found from these calculations. The dimensionless formulation of Eq. (1) is generated by appropriate scaling of the parameters. Thus the Hamiltonian is scaled by V_0; the coordinates are defined by $Q = x/\Delta x$ and $q_i = y_i/\Delta x$, and the frequencies and time are measured in units of the scaling frequency Ω, defined by $\Omega^2\Delta x^2 = V_0$.

As we show in Subsection II B, the 1D potential along the reaction coordinate with which we will operate in practice is, however, not $V_{1D}(Q)$ but the adiabatic potential $V_{ad}(Q)$, defined from Eq. (1) along the trajectory[1,19]

$$\partial V(Q,\{q\})/\partial\{q\} = 0. \quad (2)$$

This potential governs the dynamics and justifies the choice of the coordinates (x,{y}) as our basis. We show in the Appendix that, if the coupling to antisymmetric modes is weak, $V_{1D}(Q)$ and $V_{ad}(Q)$ have the same shape, but the barrier height of $V_{ad}(Q)$ is smaller than unity (in dimensionless units) as specified later. The width and height of the adiabatic potential, along with its curvatures ω_0 and $|\omega^*|$ in the minimum and at the top, respectively, are thus directly obtained from the above calculations at the stationary configurations. Its shape in the intermediate region is obtained by interpolation using the calculated curvatures; in previous studies we have shown that this shape is well represented by an analytical function of the quartic type $-ax^2 + bx^4$, which we therefore adopt in the present study.

This Hamiltonian is the logical extension of the standard "harmonic" Hamiltonian used for molecules with potentials without multiple minima, in which anharmonic terms are generally neglected. The presence of a double minimum implies an "anomalous" coordinate Q corresponding to the reaction coordinate of transition state theory. This coordinate will be

coupled to all 3N−7 normal coordinates q_i. Since $(Q, \{q\})$ are the normal modes of the TS, kinematic couplings, as well as couplings $q_i q_j$ vanish at the top of the barrier; they will thus remain small near this most important region, where Q coincides with the instanton. Therefore the 1D double-minimum potential $V_{\rm ad}(Q)$, which connects the minima, will be a good zero-order approximation. The lowest-order (linear) coupling terms allowed by symmetry will adjust the equilibrium positions of the q_i. The associated frequency changes of these modes would require quadratic coupling terms, which cannot be directly handled by the formalism. However, their principal effect, namely modifying (i.e., lowering) the barrier height, we include by the recalibration of the constants γ_i, as indicated above. The effect of rotation is neglected in Hamiltonian (1) as usual, but all parameters are calculated so that the Eckart conditions are obeyed. This is necessary in order to conserve the linear and angular momenta and thus prevent mixing of the vibrations with translations or rotations; details can be found in the Appendix and in Ref. 3. The validity of this Hamiltonian has been demonstrated by numerous applications of the AIM/DOIT approach.[2,3,12–14] It is especially well suited for proton-transfer in hydrogen bonds, where, as we show below, the most strongly coupled modes of the hydrogen bridge tend to be shifted towards the adiabatic limit, so that the adiabatic potential $V_{\rm ad}(Q)$, which is the main term of the MD potential, adequately represents the main effect of the coupling.

B. The Euclidean action

The tunneling dynamics at zero-temperature ($T = 0$) is governed by the Euclidean action evaluated along the "instanton trajectory." In particular, the zero-level tunneling splitting is given by[1]

$$\Delta E_0 = \mathcal{A} \exp(-S_{\rm E}), \tag{3}$$

where the pre-exponential $\mathcal{A}$ will be specified in Sec. IV and $S_{\rm E}$ is the Euclidean action at $T = 0$,

$$S_{\rm E} = \int_{-\infty}^{\infty} d\tau\, H[Q(\tau), \{q(\tau)\}], \tag{4}$$

evaluated along the "instanton trajectory" $[Q(\tau), \{q(\tau)\}]_{\rm I}$ that satisfies the "instanton equation," i.e., the equation of motion

$$\delta S_{\rm E} = 0. \tag{5}$$

The Hamiltonian (1) allows integration over the coupled-mode coordinates $\{q\}$,[19] for which the above equation corresponds to that of forced harmonic oscillators. The instanton action and equation then assume the well-known forms[1,19]

$$S_{\rm E} = \int_{-\infty}^{\infty} d\tau \left[\frac{1}{2}\dot{Q}^2 + V_{\rm ad}(Q)\right] + S_{\rm nl}; \quad \delta S_{\rm E}/\delta Q = 0. \tag{6}$$

Here $V_{\rm ad}(Q)$ is defined from Eqs. (1) and (2) and the nonlocal term $S_{\rm nl}$ may contain symmetric as well as antisymmetric parts, governed by the corresponding exponential (memory) kernels $U_{\rm s,\,a}$:

$$\begin{aligned} S_{\rm nl} &= S_{\rm nl,s} + S_{\rm nl,a}, \\ S_{\rm nl,s} &= \int_{-\infty}^{\infty} d\tau\, \dot{\Lambda}_{\rm s} \int_{-\infty}^{\infty} d\tau'\, \dot{\Lambda}_{\rm s} U_{\rm s}(\tau - \tau'), \\ S_{\rm nl,a} &= \int_{-\infty}^{\infty} d\tau\, \dot{\Lambda}_{\rm a} \int_{-\infty}^{\infty} d\tau'\, \dot{\Lambda}_{\rm a} U_{\rm a}(\tau - \tau'), \\ U_{\rm s,a}(\tau - \tau') &= \sum_{i={\rm a,s}} \alpha_i \exp(-\omega_i|\tau - \tau'|); \quad \alpha_i = \gamma_i^2/4\omega_i^3. \end{aligned} \tag{7}$$

In the Hamiltonian (1) we will consider potentials with only lowest-order coupling terms, viz., $\Lambda_{\rm a}(Q) = -Q$ and $\Lambda_{\rm s}(Q) = -Q^2$. We recall that the 1D tunneling potential $V_{\rm 1D}(Q)$ in Eq. (1) is the potential evaluated with the coupled oscillators $\{q\}$ frozen in their equilibrium positions. In the Appendix we show that for this choice of $V_{\rm 1D}(Q)$, provided the antisymmetric coupling is weak, the two 1D potentials are related by

$$V_{\rm ad}(Q) = (1 - B)V_{\rm 1D}(Q), \tag{8}$$

where B comprises the collective effect of the couplings on the 1D potential,

$$B = B_{\rm a} + B_{\rm s}, \quad B_{\rm a,s} = \sum_{i={\rm a,s}} \gamma_i^2/2\omega_i^2; \quad B_{\rm a} \ll B_{\rm s}. \tag{9}$$

It follows immediately from Eq. (8) that for any meaningful problem $B < 1$; otherwise the adiabatic barrier will vanish. The Euclidean action (6) thus represents a tunneling problem where the coupling to modes $\{q\}$ has a two-fold effect. First, there is a "local" effect, whereby the tunneling potential is transformed from $V_{\rm 1D}(Q)$ to $V_{\rm ad}(Q)$, i.e., to a potential with barrier height reduced from 1 to $1 - B$ (in dimensionless units), which has a promoting effect. Second, a nonlocal term $S_{\rm nl}$ enters, which can be shown to be always positive and to have a suppressing effect that reflects the "memory" (inertia) of the subsystem of coupled oscillators. The collective parameter B is the main measure of the coupling strength. It also imposes a characteristic time scale on Eq. (6): $\tau^* = 1/\sqrt{1 - B}$ (or, equivalently, the imaginary frequency under the adiabatic barrier $|\omega^*| \sim \sqrt{1 - B}$), which qualitatively defines the modes ω_i as "fast" or "slow," depending on whether $\omega_i\tau^*$ is larger or smaller than unity, respectively. It also indicates that the nonlocal contribution of modes with $\omega_i\tau^* \geq 1$ will be small.

For MD systems in general, the instanton equation (6) cannot be solved unless approximations are introduced for the nonlocal term. To this end, as mentioned in the Introduction, the "fast" coupled modes are usually treated in the AA and the "slow" modes in the SA.[1,19] In dimensionless units, this formally means replacing the exponential kernel $\exp(-\omega_i|\tau - \tau'|)$ by a delta function $(2/\omega_i)\delta(|\tau - \tau'|)$ for $\omega_i\tau^* \gg 1$; and by the leading terms of its expansion over a small $\omega_i|\tau - \tau'|$ for $\omega_i\tau^* \ll 1$. Hereafter we refer to this treatment of the kernels as the "standard approach". As indicated in the Introduction, for strong coupling this method is not always satisfactory. For this situation we therefore present an alternative approach based on a new approximation scheme, termed the rainbow approximation.

Historically, attention was focussed mostly on antisymmetric coupling, which causes friction (more generally, reorganizational effects).[20] However, calculations on molecular systems have shown that symmetric coupling, which tends to dominate tunneling in these systems, e.g., in the form of proton transfer along hydrogen-bond bridges, may have much larger effects, namely in cases where vibrations of the attached heavier atoms modulate the transfer distance.[12,13] To account for these effects in MD systems, we adopt here a two-step procedure based on the notion that in such systems the antisymmetric coupling is usually much weaker and can be incorporated by rescaling of variables and parameters. In the first step, covered by Subsection II C, we therefore deal exclusively with symmetric coupling. In the second step, discussed in Sec. III C, we show how to incorporate (weak) antisymmetric coupling.

C. The symmetric nonlocal action

In this subsection, we limit ourselves to coupling with symmetric modes only. We are mainly interested in strong symmetric coupling, and to provide some background information, we list in Table I values of some of the parameters introduced above for hydrogen-bonded molecules and complexes for which such information has been reported. In particular, we note that the collective coupling parameter B, which for these systems is dominated by the symmetric coupling parameter B_s, tends to be in the range 0.5–0.7 with frequencies of the dominant modes of order $\omega_i/\sqrt{1-B_s} \sim 1$. In this range the standard approach performs poorly.[19,21]

TABLE I. Main dynamics parameters of proton transfer in the hydrogen-bonded systems considered here and in Part II: Δx, half the barrier width defined in Eq. (A9) (mass-weighted, in Å·(amu)$^{1/2}$); V_0 and U_0, barrier height along the LRP and at the TS, respectively (in kcal/mol); ω_0 and $|\omega^*|$, frequency along the reaction coordinate in the well and at the TS, respectively (in cm^{-1}); B, collective coupling parameter defined in Eqs. (8) and (9); $\Delta E_0^{\rm obs}$, observed zero-level tunneling splitting (in cm^{-1}). The level of calculation for malonaldehyde (MA-d_0/d_1) is specified in Sec. VI; for the other systems details will be given in Part II. Note that in MA-d_0/d_1 the observed zero-level splitting is attributed to single-proton tunneling; in porphycene (PHC), the benzoic acid dimer (BAD), the formic acid dimer (FAD) and the 2-pyridone-2-hydroxypyridine (2PH) complex, to concerted double-proton tunneling, and in calix[4]arene (CLX) to concerted quadruple-proton transfer, with correspondingly increasing U_0 and decreasing $\Delta E_0^{\rm obs}$.

Molecule	Δx	ω_0	$\lvert\omega^*\rvert$	U_0	V_0	B	$\Delta E_0^{\rm obs}$
MA-d_0	0.430	2642	1384	4.08	14.44	0.72	21.6[a]
MA-d_1	0.571	1940	1036	4.08	14.44	0.72	2.9[b]
PHC	0.495	2027	1024	4.08	8.76	0.53	4.4[c]
BAD	0.585	2749	1255	7.33	21.43	0.66	0.037[d]
FAD	0.585	2946	1430	7.93	27.60	0.71	0.016[e]
2PH	0.596	2759	1310	8.35	24.26	0.65	0.017[f]
CLX	0.727	2835	1448	16.86	30.05[g]	0.44	—

[a]Reference 23.
[b]Reference 24.
[c]Reference 31.
[d]Reference 32.
[e]Reference 17.
[f]Reference 33.
[g]$U_0 + E_r$, defined in Eq. (A14).

Equally unsatisfactory are perturbative approaches of the type developed for the "strong fluctuation limit",[6] when B_s is so large that $\sqrt{1-B_s} \ll 1$. We therefore propose an alternative approach, based on the notion that the nonlocal term $S_{\rm nl,s}$ in Eq. (7) is relatively small even if the coupling is strong. This follows from the observation that such coupling "shifts" the most strongly coupled modes towards the "fast" group $\omega_i\tau^* \geq 1$, whereby the exponential kernels defined in Eq. (7) fall-off rapidly. Such terms need not be treated exactly, but can be evaluated with some suitable approximate instanton solution $Q^{(0)}(\tau) \simeq Q(\tau)$, while the exponential kernels are kept intact. The nonlocal part of the action $S_{\rm E}$ is thus replaced by a constant: $S_{\rm nl,s}^{(0)} \simeq S_{\rm nl,s}$, in which case Eq. (6) yields the instanton action in the form

$$S_{\rm E,s} = S_{\rm ad} + S_{\rm nl,s}^{(0)}, \tag{10}$$

where the main term $S_{\rm ad}$ is the instanton action of 1D-motion in the adiabatic potential,

$$S_{\rm ad} = S_{\rm 1D}\sqrt{1-B_{\rm s}}; \quad S_{\rm 1D} = \int_{-1}^{1} dQ\sqrt{2V_{\rm 1D}(Q)}, \tag{11}$$

and the nonlocal (correction) term is given by

$$S_{\rm nl,s}^{(0)} = \int_{-\infty}^{\infty} d\tau\,\dot{\Lambda}^{(0)} \int_{-\infty}^{\infty} d\tau'\dot{\Lambda}^{(0)}\,U_{\rm s}(\tau-\tau'),$$
$$\Lambda^{(0)}(\tau) = 1 - [Q^{(0)}(\tau)]^2, \tag{12}$$

$U_{\rm s}(\tau-\tau')$ being the exponential kernel defined in Eq. (7). Since $S_{\rm nl,s}$ is positive but presumed small, it makes sense to start from $S_{\rm ad}$ as the lower limit to $S_{\rm E,s}$ and look for a suitable approximate solution $Q^{(0)}(\tau)$. The type of this solution is dictated by the "shift" of the most strongly coupled mode towards the "fast" group, as defined above. One may therefore expect that a "good enough" approximate solution can be found by separating the modes into "fast" and "slow," so that this most important mode is treated in the AA; the remaining (weakly coupled) modes can be treated in the AA or in the SA, based (qualitatively) on whether the ratio $\omega_i/\sqrt{1-B_s}$ is larger or smaller than unity. This "rainbow" solution, so termed because it covers a wide range of frequencies, will be our approximate solution of choice for the evaluation of the nonlocal term in Eq. (12).

The advantage of the proposed scheme is two-fold: first, the approximation involved in Eq. (12), whereby Λ is replaced by $\Lambda^{(0)}$ while the kernels are kept intact, proves to be much less drastic than the standard approach; and second, any ambiguity in assigning a mode to the "fast" or the "slow" group affects only the (small) nonlocal action and leaves the main adiabatic action untouched. However, for MD systems, $Q^{(0)}(\tau)$ is known only in numerical form; as a result, evaluation of the action (12) is not a trivial task since it contains double integrations, each over terms of the type $Q^{(0)}(\tau)\dot{Q}^{(0)}(\tau)$, such that the multipliers tend to cancel each other. To overcome this problem, we take advantage of a remarkable "conversion property" of our chosen form of $Q^{(0)}(\tau)$, namely the fact that, even though $Q^{(0)}(\tau)$ is numerical, the inverse function $\tau = \tau(Q^{(0)})$ is *analytical* for the quartic shape of the adiabatic potential in Eq. (6). This property allows us to reformulate the integration in Eq. (12) in terms of $(\Lambda^{(0)}, \Lambda^{(0)'})$, instead

of (τ, τ') by recasting the solution in the form of the exponent of the kernel in Eq. (7). Thus, breaking the integrations in Eq. (12) so that $(\tau, \tau') \geq 0$ and introducing

$$\exp(\mp\omega_i \tau) = \phi_i^{\pm}(\Lambda^{(0)}), \tag{13}$$

we recast Eq. (12) in the following general form (the integration limits remain unspecified):

$$S_{\mathrm{nl,s}}^{(0)} = \int d\Lambda^{(0)} \int d\Lambda^{(0)'} U_s(\Lambda^{(0)}, \Lambda'^{(0)}),$$
$$U_{\mathrm{s}}(\Lambda^{(0)}, \Lambda'^{(0)}) = \sum_{i=\mathrm{s}} \alpha_i \phi_i^{+}(\Lambda^{(0)}) \phi_i^{-}(\Lambda'^{(0)}), \tag{14}$$

which allows a very efficient computational procedure, since the functions $\phi_i^{\pm}(\Lambda^{(0)})$ are *analytical* expressions. The evaluation of the nonlocal action (12) thus becomes much more efficient, and the presentation is altogether more appealing.

To illustrate the approach, we consider a 2D model of a quartic potential coupled symmetrically to a single mode; henceforth, we shall refer to it as the 2D quartic model. The 1D potential $V_{\mathrm{1D}}(Q)$, the Hamiltonian, and the action S_{1D} in Eq. (11) are then given by

$$V_{\mathrm{1D}}(Q) = (1 - Q^2)^2; \quad H = \frac{1}{2}\dot{Q}^2 + \frac{1}{2}\dot{q}_s^2 + (1 - Q^2)^2$$
$$- \gamma_s Q^2 q_s + \frac{1}{2}\omega_s^2 q_s^2; \quad S_{\mathrm{1D}} = (4/3)\sqrt{2}. \tag{15}$$

The nonlocal action in Eqs. (6)–(8) contains a single (symmetric) term, ω being the frequency of the coupled mode and α the coefficient of the kernel. We evaluate $S_{\mathrm{nl,s}}^{(0)}$ using as an approximate instanton solution the "zero-order" solution $Q^{(0)}(\tau)$ obtained when the nonlocal action in Eq. (6) is simply neglected. This is the instanton solution for the action in the main part of Eq. (6), where $V_{\mathrm{ad}}(Q) = (1 - B_{\mathrm{s}})(1 - Q^2)^2$, which is known analytically,[1]

$$Q^{(0)}(\tau) = \tanh\left[\tau\sqrt{2(1 - B_{\mathrm{s}})}\right]. \tag{16}$$

For $\tau \geq 0$ the exponents of the kernel take the analytical form

$$\exp(\mp\omega\tau) = \left[\Lambda^{(0)}/\left(1 + \sqrt{1 - \Lambda^{(0)}}\right)^2\right]^{\pm\xi} = \phi^{\pm}(\Lambda^{(0)}),$$
$$\xi = \omega/2\sqrt{2(1 - B_{\mathrm{s}})}. \tag{17}$$

Hence the transformation leading to Eq. (14) can now be carried out explicitly. Breaking the integrals in Eq. (12) so that $(\tau, \tau') \geq 0$, and taking advantage of the above presentation of the exponents, we obtain $S_{\mathrm{nl,s}}^{(0)}$ in the form of simple quadratures (z denotes $\Lambda^{(0)}$ or $\Lambda'^{(0)}$):

$$S_{\mathrm{nl,s}}^{(0)} = 2\alpha\mathcal{C}(\phi^{\pm}); \quad \mathcal{C}(\phi^{\pm}) = -I_1^2(0, 1)$$
$$+ \int_0^1 dz[\phi^{+}(z) I_2(z, 1) + I_1(0, z)\phi^{-}(z)],$$
$$I_1(a, b) = \int_a^b dz\, \phi^{+}(z); \quad I_2(a, b) = \int_a^b dz\, \phi^{-}(z), \tag{18}$$

where $\mathcal{C}$ is a constant; these integrals are readily evaluated numerically.

Returning to our problem leading to Eq. (14), we show in Sec. III that the rainbow instanton solution, described above, leads to a similar transformation of the integrals. Since many coupled modes are now present, the nonlocal action takes the form of a sum-over-modes of expressions similar to the one above, but with the contribution of each single mode scaled down by the contributions of all the other coupled modes. We will show that the scaling factor is determined by $Q_0 = Q^{(0)}(\tau \to \infty)$, the final result being

$$S_{\mathrm{nl,s}}^{(0)} = 2Q_0^4 \sum_{i=\mathrm{s}} \alpha_i \mathcal{C}(\phi_i^{\pm}); \quad Q_0 = Q^{(0)}(\tau \to \infty) \leq 1, \tag{19}$$

where α_i are the kernel coefficients in Eq. (7) and the functions $\phi_i^{\pm}(x)$ are defined by the rainbow solution $Q^{(0)}(\tau)$. The specific form of the functions $\mathcal{C}(\phi_i^{\pm})$ and the value Q_0, evaluated by a simple numerical procedure, are derived in Sec. III. The numerical problem of evaluating the nonlocal action is thus reduced to simple quadratures over "well-behaved" functions, the key being that the functions $\phi_i^{\pm}(x)$ are known analytically. The instanton action is then obtained from Eqs. (10), (11), and (19). This procedure remains valid if antisymmetric coupling is included, provided this coupling is weak. In that case it can be formally incorporated by rescaling the variables and the parameters of symmetric coupling. A full justification of the statements is provided in Sec. III.

III. THE RAINBOW APPROXIMATION

In this section, we provide a detailed mathematical justification of the results of Sec. II. In Sec. III A, we outline the derivation of the rainbow solution and Eq. (19) for arbitrary double-minimum potentials. To be specific and allow comparison with model results, we present explicit formulas for the quartic potential. In Sec. III B, we define a heuristic model, in which all relations of Sec. III A can be simplified. In Sec. III C, we reintroduce (weak) antisymmetric coupling and show how it can be incorporated by rescaling.

A. Derivation of $S_{\mathrm{nl,s}}^{(0)}$

We consider a system of the type treated in Sec. II with symmetric coupling only and with both "fast" and "slow" modes based on a specified separation criterion. First, we obtain the desired approximate solution $Q^{(0)}(\tau)$ by solving the problem defined by Eqs. (6) and (7), to which we apply the standard approach, i.e., we treat the exponential kernels in the AA for the "fast," and in the SA for the "slow" modes, as prescribed in Sec. II B. As is well known,[6] the corresponding nonlocal terms renormalize the mass and the potential, respectively. To simplify the notation, we use single and double primes to denote parameters for "fast" and "slow" modes, respectively, and write

$$B_{\mathrm{s}} = B' + B'', \quad B' = \sum_{i=\mathrm{s}'} B_i, \quad B'' = \sum_{i=\mathrm{s}''} B_i,$$
$$B_i = \gamma_i^2/2\omega_i^2, \quad B_{\mathrm{eff}} = B''/(1 - B'), \quad A_{\mathrm{s}} = A' + A'',$$
$$A' = \sum_{i=\mathrm{s}'} A_i, \quad A'' = \sum_{i=\mathrm{s}''} A_i, \quad A_i = \gamma_i^2/4\omega_i,$$
$$A_{\mathrm{eff}} = A''/(1 - B')^{3/2}. \tag{20}$$

We omit the superscript (0) of Q and take $\Lambda = 1 - Q^2$. Introducing $Q_0 = Q(\infty)$, which remains to be found, we then obtain for the Euclidean action:

$$S_{\mathrm{E,s}} = \int_{-\infty}^{\infty} d\tau \left[\frac{1}{2} m_{\mathrm{eff}}(Q)\dot{Q}^2 + V_{\mathrm{eff}}(Q)\right] - A''\left(\int_{-\infty}^{\infty} d\tau \left[Q_0^2 - Q^2(\tau)\right]\right)^2, \tag{21}$$

where the renormalized mass and potential are given by

$$m_{\mathrm{eff}}(Q) = 1 + \Delta m_{\mathrm{s}} Q^2, \quad \Delta m_{\mathrm{s}} = 4\sum_{i=\mathrm{s}'} \gamma_i^2/\omega_i^4,$$
$$V_{\mathrm{eff}}(Q) = V_{\mathrm{ad}}(Q) + B''\left(Q_0^2 - Q^2\right)^2. \tag{22}$$

We start with a general analysis of the instanton equation $\delta S_{\mathrm{E}}/\delta Q = 0$, which will allow us to define Q_0; the explicit solution will follow. Introducing the new variable $t = \tau\sqrt{1 - B'}$ and the boundary conditions $\dot{Q}(t \to \pm\infty) = 0$, we rewrite the instanton equation formally as

$$\dot{Q}(t) = \sqrt{2U_{\mathcal{F}}(Q)/m_{\mathrm{eff}}(Q)}. \tag{23}$$

In this expression we have introduced the "potential" $U_{\mathcal{F}}(Q)$, defined in terms of the (unknown) functional constant

$$\mathcal{F}(Q_0) = 1 - B_{\mathrm{eff}}\left(1 - Q_0^2\right) - A_{\mathrm{eff}} \int_{-\infty}^{\infty} dt \left[Q_0^2 - Q^2(t)\right], \tag{24}$$

which for a quartic potential $V_{\mathrm{ad}}(Q) = (1 - B_{\mathrm{s}})(1 - Q^2)^2$ takes the analytical form

$$U_{\mathcal{F}}(Q) = [\mathcal{F}(Q_0) - Q^2]^2. \tag{25}$$

The formal "solution" of this equation, in the form of the integral

$$t = \frac{1}{\sqrt{2}} \int dQ \sqrt{m_{\mathrm{eff}}(Q)}/|\mathcal{F}(Q_0) - Q^2| \tag{26}$$

can be obtained analytically for any $\mathcal{F}(Q_0)$, because it is a positive constant. The result $t = t_{\mathcal{F}}(Q)$ has the correct asymptotic behavior $t \to \pm\infty$ at $Q \to \pm Q_0$ only if $\mathcal{F}(Q_0) = Q_0^2$. From Eqs. (25) and (26) we then obtain a closed relation for Q_0, as follows:

$$Q_0^2 = 1 - B_{\mathrm{eff}}\left(1 - Q_0^2\right) - (A_{\mathrm{eff}}/\sqrt{2})I(Q_0),$$
$$I(Q_0) = \int_{-Q_0}^{Q_0} dz\sqrt{1 + \Delta m_{\mathrm{s}} z^2} = Q_0\sqrt{1+\rho} + \sinh^{-(\sqrt{\rho})}/\sqrt{\Delta m_{\mathrm{s}}}; \quad \rho = \Delta m_{\mathrm{s}} Q_0^2, \tag{27}$$

which can be solved numerically for Q_0. With Q_0 and $\mathcal{F}(Q_0)$ defined, the solution of the instanton equation (26) can then be readily obtained for any system that contains both "fast" and "slow" modes. For that we rescale to $\bar{Q} = Q/Q_0$, $\bar{t} = \tau Q_0\sqrt{1 - B'}$ and $m_{\mathrm{eff}}(\bar{Q}) = 1 + \rho\bar{Q}^2$ to obtain the solution in a form that is convenient for our purpose,

$$\bar{t} \equiv \bar{t}(\bar{Q}) = \sigma^{-1} \ln \frac{g + \sqrt{1+g^2}}{(f + \sqrt{1+f^2})^{\kappa}}, \tag{28}$$

here the functions f and g, and the constants κ and ρ are given by

$$f(\bar{Q}) = 2\bar{Q}\sqrt{\rho m_{\mathrm{eff}}(\bar{Q})}, \quad g(\bar{Q}) = f(\bar{Q})/\kappa(1 - \bar{Q}^2),$$
$$\kappa = \sqrt{\rho/(1+\rho)}, \quad \sigma = 2\sqrt{2}/\sqrt{(1+\rho)}. \tag{29}$$

This is the rainbow solution, which is so named because it reproduces the known "slow-flip" and "fast-flip" solutions, when all modes are "fast" and when all modes are "slow," respectively (which can be regarded as the "blue" and "red" edges of the rainbow), as well as interpolating smoothly between those limits if both types of modes are present. Corresponding solutions, albeit not in analytical form, can be obtained for potentials other than the quartic potential.

At $\bar{t} \geq 0$, the rhs of Eq. (28) is a function of $\bar{\Lambda} = 1 - \bar{Q}^2$ only. This immediately leads to the desired "conversion property" (13) [superscripts (0) at $\bar{\Lambda}$ omitted], since the exponential kernels $\exp(\mp\omega_i\tau)$ can now be evaluated if we set $\bar{t} = \bar{t}(\bar{\Lambda})$,

$$\exp(\mp\omega_i\tau) = \exp[\mp\nu_i\bar{t}(\bar{\Lambda})] \equiv \phi_i^{\pm}(\bar{\Lambda}),$$
$$\phi_i^{\pm}(\bar{\Lambda}) = \left[\frac{g + \sqrt{1+g^2}}{\left(f + \sqrt{1+f^2}\right)^{\kappa}}\right]^{\pm\xi_i}, \tag{30}$$

where $\xi_i = \nu_i/\sigma$ and $\nu_i = \omega_i/Q_0\sqrt{1 - B'}$. With the exponents defined, we are now in a position to transform the integration over (τ, τ') for the nonlocal term in Eq. (14) to an integration over $(\bar{\Lambda}, \bar{\Lambda}')$. This yields the final result in the form of Eq. (19), which reads

$$S_{\mathrm{nl,s}}^{(0)} = 2Q_0^4 \sum_{i=\mathrm{s}} \alpha_i \mathcal{C}(\phi_i^{\pm}),$$
$$\mathcal{C}(\phi_i^{\pm}) = -I_{1i}^2(0,1) + \int_0^1 dz[\phi_i^+(z)I_{2i}(z,1) + I_{1i}(0,z)\phi_i^-(z)], \tag{31}$$
$$I_{1i}(a,b) = \int_a^b dz\,\phi_i^+(z); \quad I_{2i}(a,b) = \int_a^b dz\phi_i^-(z).$$

Here α_i are the kernel coefficients in Eq. (7). Despite the cumbersome appearance, the above sum is readily obtained numerically, since the functions $\phi_i^{\pm}(z)$ are known analytically.

B. A heuristic model

The transformation $\exp(\mp\omega_i\tau) \equiv \phi_i^{\pm}(\bar{\Lambda})$ in Eq. (30), whose merits are masked by the complicated form of the solution (28), becomes much more transparent if written in the form $\exp(-\sigma|\bar{t}|)$, in which form it can be very well approximated by the following function:

$$\exp(-\sigma|\bar{t}|) \simeq \exp(-\sigma|\bar{t}|)^{(\mathrm{M})} = \bar{\Lambda}\exp\left(-\epsilon\sqrt{1 - \bar{\Lambda}}\right),$$
$$\epsilon = (1 - \kappa)[\kappa + \ln 4(1+\rho)]. \tag{32}$$

This defines a heuristic model to our solution, hereafter labeled by a superscript (M). Figure 1 shows the behavior of the rainbow solution (28), depicted in the form of the exponent $\exp(-\sigma|\bar{t}|)$ for parameter values derived for the molecule malonaldehyde discussed in Sec. VI. It also depicts the model

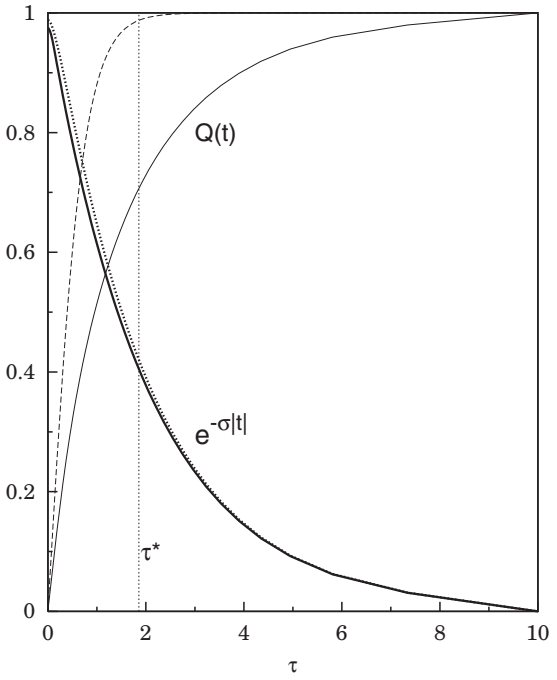

FIG. 1. Illustration of the rainbow solution (28) for malonaldehyde-d_0 discussed in Sec. VI, where all coupled modes are "fast" and therefore the rainbow solution is simply the "slow-flip" solution. The thick solid line represents this solution in the form of the exponent $\exp(-\sigma|t|)$, where $t = \tau/\tau^*$; $\tau^* = \sqrt{1-\widetilde{B}_s}$. The thick dotted line represents its model counterpart given by Eq. (32). The thin solid line represents this solution in the standard form $Q(\tau)$, in comparison with the "zero-order" solution of Eq. (16) (thin dashed line), obtained by neglecting the nonlocal term in the action; only $Q(\tau \geq 0)$ is shown, $Q(-\tau) = -Q(\tau)$. Parameters (see Sec. III C and Tables I and IV): $\widetilde{B}_s = 0.710$, $\Delta m_s = 8.657$, $Q_0 = 1$, $\sigma = 0.910$, $\epsilon = 0.245$.

of Eq. (32), which is in excellent agreement with the exact result. The figure depicts the rainbow solution also in the standard form $Q(\tau)$, on the time scale of tunneling τ^*. Comparison with the zero-order solution of Eq. (16), (also shown in Fig. 1), in which the nonlocal term of the Euclidean action is neglected, illustrates the effect of this term.

Within this model, the evaluation of $S^{(0)}_{\mathrm{nl,s}}$ becomes much simpler, and the presentation much more transparent, since the exponents (30) and the transformation of the integrals, leading to Eq. (14), are similar to those for the 2D quartic model used in Sec. II C for illustration. Thus (for $\tau \geq 0$)

$$\exp(\mp\omega_i\tau) \simeq \phi_i^{(\mathrm{M})\pm}(\bar{\Lambda}) = [\bar{\Lambda}\exp(-\epsilon\sqrt{1-\bar{\Lambda}})]^{\pm\xi_i}. \tag{33}$$

The transformation of the integrals, leading to Eq. (14) can be carried out explicitly. Noting that $d\Lambda^{(0)} = Q_0^2 d\bar{\Lambda}$ and that the limits $\tau \in (0,\infty)$ transform into $\bar{\Lambda} \in (1,0)$, respectively, we obtain the nonlocal action in the form of simple quadratures,

$$S^{(0)}_{\mathrm{nl,s}} \simeq S^{(\mathrm{M})}_{\mathrm{nl,s}} = 2Q_0^4 \sum_{i=\mathrm{s}} \alpha_i \mathcal{C}_i^{(\mathrm{M})},$$

$$\mathcal{C}_i^{(\mathrm{M})} = \frac{1}{\xi_i+1} + \epsilon\frac{2\xi_i}{\xi_i-1}\left(J_{1i} - \frac{2J_0}{\xi_i+1}\right) - J_{2i}^2,$$

$$J_0 = \int_0^1 dz\,(z\sqrt{1-z}) = 4/15,$$

$$J_{1i} = \int_0^1 dz\,(z^{\xi_i}\sqrt{1-z}),$$

$$J_{2i} = \int_0^1 dz\,[z\exp(-\epsilon\sqrt{1-z})]^{\xi_i}. \tag{34}$$

For any given MD system, this (model) approximation to the nonlocal action is easily evaluated, since the relevant parameters are readily available, without further reference to the details of the rainbow solution. This provides, for instance, a transparent way to obtain a quick and sound estimate of the tunneling splitting, as we show later.

C. Antisymmetric modes

Although for the systems to be considered, the coupling is predominantly symmetric, antisymmetric coupling is not absent and needs to be addressed; we therefore return to the general formulation of the Euclidean action in Eqs. (6)–(9). For the purpose of the present study, which deals primarily with strong symmetric coupling, this coupling is weak: $B_a \ll B_s$, such that it can be treated with the standard approach. To this end we again separate the modes $\{q_a\}$ into "fast" (a') and "slow" (a") modes, and replace the exponents in the antisymmetric part of the kernel (7) by the corresponding approximations described earlier. As is well known, this leads to mass renormalization for the fast modes, represented by a constant term Δm_a to be added to the tunneling mass, and a Franck–Condon factor for the slow modes, represented by a term ΔS_a to be added to the Euclidean action; these terms take the form[6]

$$\Delta m_a = \sum_{i=a'} \gamma_i^2/\omega_i^4; \quad \Delta S_a = Q_0^2 \sum_{i=a''} \gamma_i^2/\omega_i^3, \tag{35}$$

where Q_0 is evaluated from Eq. (27). It follows that apart from adding a term ΔS_a to the action, the antisymmetric modes modify the mass and the 1D potential of the tunneling particle. These modifications transform Eq. (6) into

$$S_E = \int_{-\infty}^{\infty} d\tau \left[\frac{1}{2}(1+\Delta m_a)\dot{Q}^2 + (1-B_a-B_s)V_{1D}(Q)\right] + \int_{-\infty}^{\infty} d\tau\,\dot{\Lambda}_s \int_{-\infty}^{\tau} d\tau'\,\dot{\Lambda}_s \sum_{i=s} \alpha_i \exp[-\omega_i(\tau-\tau')] + \Delta S_a. \tag{36}$$

We can, however, recast this equation in a form that contains symmetric terms only by rescaling the parameters as follows:

$$\begin{aligned} &\widetilde{\tau} = \tau/C_1, \quad \widetilde{\omega}_i = C_1\omega_i, \quad \widetilde{\gamma}_i = C_2\gamma_i; \quad \widetilde{\alpha}_i = \widetilde{\gamma}_i^2/2\widetilde{\omega}_i^3, \\ &\widetilde{B}_s = \sum_{i=s} \widetilde{\gamma}_i^2/2\widetilde{\omega}_i^2; \quad \widetilde{A}_s = \sum_{i=s} \widetilde{\gamma}_i^2/4\widetilde{\omega}_i, \\ &C_1 = [(1+\Delta m_a)/(1-B_a)]^{1/2}, \\ &C_2 = [(1+\Delta m_a)]^{1/2}/(1-B_a). \end{aligned} \tag{37}$$

The Euclidean action then assumes the form

$$S_E = C_a\widetilde{S}_{E,s} + \Delta S_a; \quad C_a = [(1+\Delta m_a)(1-B_a)]^{1/2}, \tag{38}$$

where $\widetilde{S}_{\mathrm{E,s}}$ is given by

$$\widetilde{S}_{\mathrm{E,s}} = \int_{-\infty}^{\infty} d\tilde{\tau}\left[\frac{1}{2}\dot{Q}^2 + (1-\widetilde{B}_{\mathrm{s}})(1-Q^2)^2\right] + \int_{-\infty}^{\infty} d\tilde{\tau}\,\dot{\Lambda}_{\mathrm{s}} \int_{-\infty}^{\infty} d\tilde{\tau}'\,\dot{\Lambda}_{\mathrm{s}} \sum_{i=\mathrm{s}} \widetilde{\alpha}_i \exp[-\widetilde{\omega}_i(\tilde{\tau}-\tilde{\tau}')]. \quad (39)$$

This expression contains only symmetric coupling and therefore the evaluation of $\widetilde{S}_{\mathrm{E,s}}$ can be done as in Sec. III A; this yields $\widetilde{S}_{\mathrm{E,s}}$ in the form of Eq. (10),

$$\widetilde{S}_{\mathrm{E,s}} = \widetilde{S}_{\mathrm{ad}} + \widetilde{S}^{(0)}_{\mathrm{nl,s}}; \quad \widetilde{S}_{\mathrm{ad}} = S_{1\mathrm{D}}\sqrt{1-\widetilde{B}_{\mathrm{s}}}, \quad (40)$$

where $\widetilde{S}^{(0)}_{\mathrm{nl,s}}$ is evaluated as detailed in Sec. III A, with the rescaled parameters (37) (marked with a tilde).

Combining Eqs. (38) and (40), we finally obtain for the instanton action

$$S_{\mathrm{E}} = C_{\mathrm{a}}\widetilde{S}_{\mathrm{E,s}} + \Delta S_{\mathrm{a}}, \quad \widetilde{S}_{\mathrm{E,s}} = \widetilde{S}_{\mathrm{ad}} + \widetilde{S}^{(0)}_{\mathrm{nl,s}}, \quad \widetilde{S}_{\mathrm{ad}} = S_{1\mathrm{D}}\sqrt{1-\widetilde{B}_{\mathrm{s}}}. \quad (41)$$

In this expression, C_{a} and ΔS_{a} represent the effect of the "fast" and "slow" antisymmetric modes, respectively, $\exp(-2\Delta S_{\mathrm{a}})$ being the familiar Franck–Condon factor in the tunneling probability.[1] Since the antisymmetric coupling is weak, $\widetilde{B}_{\mathrm{s}} \simeq B_{\mathrm{s}}$, and C_{a} and $\exp(-\Delta S_{\mathrm{a}})$ are of order unity. Note that the above action is "dimensionless", i.e., needs to be multiplied by the scaling coefficient $V_0/\hbar\Omega$ (e.g., in the evaluation of zero-level splittings).

A similar expression can be obtained for the heuristic model defined in Sec. III B when $\widetilde{S}^{(0)}_{\mathrm{nl,s}}$ is replaced by its model counterpart,

$$S^{(\mathrm{M})}_{\mathrm{E}} = C_{\mathrm{a}}\widetilde{S}^{(\mathrm{M})}_{\mathrm{E,s}} + \Delta S_{\mathrm{a}}, \quad \widetilde{S}^{(\mathrm{M})}_{\mathrm{E,s}} = \widetilde{S}_{\mathrm{ad}} + \widetilde{S}^{(\mathrm{M})}_{\mathrm{nl,s}}. \quad (42)$$

It can be used for the evaluation of zero-level splittings, for which, as we show later, it consistently provides a sound estimate.

This concludes the derivation of the instanton action S_{E} in the present scheme. We note that the approach leading to these expressions is general, although for definiteness we have used the case where $V_{\mathrm{ad}}(Q)$ assumes the form of a quartic potential such that $S_{1\mathrm{D}}(Q)$ is given by Eq. (15).

IV. THE ZERO-LEVEL TUNNELING SPLITTING

The zero-level tunneling splitting ΔE_0 is defined in Eq. (3), where the pre-exponent $\mathcal{A}$, which reflects the fluctuations around the instanton trajectory at $T = 0$, needs to be specified. This pre-exponent is generally a complex quantity which involves evaluation of determinants of differential operators.[1] If there is only one instanton path at $T = 0$, it allows factorization of the determinants into "longitudinal" (l) and "transverse" (t) factors, defined by the properties of motion along the instanton and the coordinates perpendicular to it, respectively. Following Ref. 22, we can then write ΔE_0 as the product of the "one-dimensional" (longitudinal) tunneling splitting $\Delta E^{(\mathrm{l})}_0$ in the potential along the instanton trajectory, and a transverse factor Γ_{t} at $T = 0$:

$$\Delta E_0 = \Delta E^{(\mathrm{l})}_0 \Gamma_{\mathrm{t}}. \quad (43)$$

Here the longitudinal tunneling splitting $\Delta E^{(\mathrm{l})}_0$ is of the general form

$$\Delta E^{(\mathrm{l})}_0 = \sqrt{2S_{\mathrm{E}}/\pi}\,\Gamma_{\mathrm{l}} \exp(-S_{\mathrm{E}}), \quad (44)$$

where S_{E} is the instanton action and Γ_{l} a "longitudinal" factor which depends on the shape of the potential along the extreme path. The "transverse" factor is given by

$$\Gamma_{\mathrm{t}} = \lim_{\beta\to\infty} \prod_{i=\mathrm{t}} \left[\frac{\sinh(\beta\omega_{0i}/2)}{\sinh(\lambda_i/2)}\right]^{1/2}, \quad (45)$$

where $\beta = 1/k_B T$, $\{\omega_{0i}\}$ are the frequencies of the transverse modes at the minimum and λ_i is a "stability parameter" which indicates to what extent the transverse mode q_i can cause deviation from the instanton trajectory. The pre-exponent $\mathcal{A}$ is thus defined in the general form as

$$\mathcal{A} = \sqrt{2S_{\mathrm{E}}/\pi}\,\Gamma_{\mathrm{l}}\Gamma_{\mathrm{t}}. \quad (46)$$

There is at present no practical way to calculate Γ_{t} for an MD system at reasonable computational cost. In our AIM/DOIT approach we evaluated this factor in the adiabatic approximation for the transverse modes, which leads to renormalization of the adiabatic barrier.[3,12,13] Recently, Mil'nikov and Nakamura[9] proposed a promising approach, using transformation to Jacobi fields, thus avoiding approximations about the properties of the transverse modes. Benderskii and Makarov[21] have carried out calculations for a two-dimensional model potential in which the transverse modes are represented by a single "effective" symmetric mode. Although these results can be applied to the MD systems under discussion (*vide infra*), a simpler and more general approach is desirable. Since inaccuracies in the pre-exponential factor $\mathcal{A}$ affect the calculated splitting much less severely than inaccuracies in the exponent S_{E}, it seems justified to evaluate $\mathcal{A}$ by a simpler scheme than that used for S_{E}. Within the present approach, a straightforward simplification is available, based on the fact that $\widetilde{S}_{\mathrm{ad}}$ is the main part of the instanton action in Eq. (40), all remaining terms being small corrections. Since by definition $\widetilde{S}_{\mathrm{ad}}$ is the instanton action of 1D motion in the adiabatic potential $V_{\mathrm{ad}}(Q)$, which is in the shape of the quartic potential (15), we adopt the expression found for this potential,[1]

$$\mathcal{A} = (\hbar\omega_0/\pi)\sqrt{24\pi S_{\mathrm{E}}}, \quad (47)$$

where ω_0 is the (dimensional) frequency along the reaction coordinate in the potential well.

The expression for ΔE_0 to be used in the present study (and in Part II) thus takes the final form

$$\Delta E_0 = (\hbar\omega_0/\pi)\sqrt{24\pi S_{\mathrm{E}}}\,\exp(-S_{\mathrm{E}}), \quad (48)$$

where the final form of the Euclidean action, which includes the scaling coefficient $V_0/\hbar\Omega$, is given by

$$S_{\mathrm{E}} = (V_0/\hbar\Omega)\left[C_{\mathrm{a}}\left(\widetilde{S}_{\mathrm{ad}} + \widetilde{S}^{(0)}_{\mathrm{nl,s}}\right) + \Delta S_{\mathrm{a}}\right], \quad \widetilde{S}_{\mathrm{ad}} = S_{1\mathrm{D}}\sqrt{1-\widetilde{B}_s}. \quad (49)$$

Here $S_{1\mathrm{D}}$ is given by Eq. (15) and the other parameters are defined in Sec. III; specifically, $\widetilde{B}_{\mathrm{s}}$ by Eq. (37); C_{a} by Eq. (38); ΔS_{a} by Eq. (35), and $\widetilde{S}^{(0)}_{\mathrm{nl,s}}$ is of the form of Eq. (31),

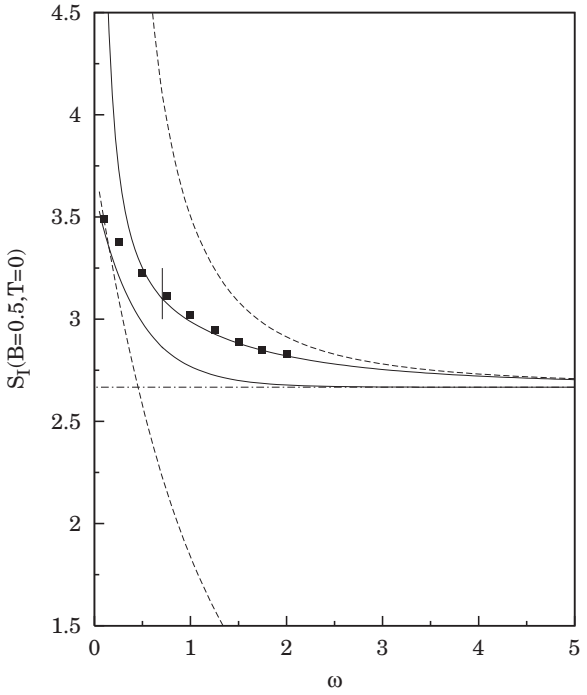

FIG. 2. Periodic-orbit action $S_I(T = 0)$ for the model 2D system of Sec. V, which consists of a quartic potential coupled symmetrically to a harmonic oscillator, for $B = 0.5$ and varying ω. The symbols represent the results of Benderskii and Makarov.[21] The upper//lower dashed lines represent the "slow flip"//"fast flip" results of Eq. (50). The dot-dash line represents the main term $S_{I,ad} = (8/3)\sqrt{2(1-B)}$ of our solution given by Eq. (52), and the upper//lower solid lines depict its limits $S_I^{AA}//S_I^{SA}$. The short vertical line indicates $1/\tau^* = \sqrt{1-B}$; all parameters are dimensionless.

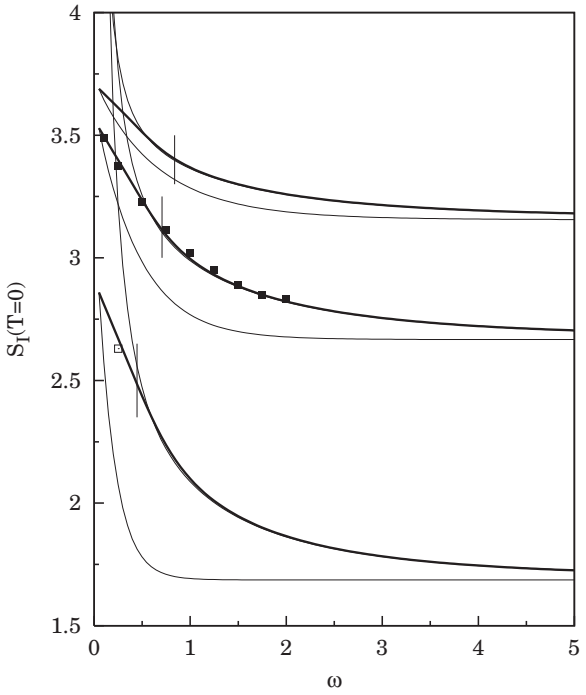

FIG. 3. Same as in Fig. 2, for $B = 0.8$ (lowest set); $B = 0.5$ (middle set), and $B = 0.3$ (upper set). The symbols represent the results of Benderskii and Makarov.[21] The thick solid lines represent the result of linear interpolation between $S_I^{AA}(\omega \simeq \sqrt{1-B})$ and $S_I^{SA}(\omega \ll 1)$.

but is evaluated with the rescaled parameters (marked with a tilde) of Eq. (37).

As we show in Sec. V, this approach yields very good agreement with known instanton solutions for 2D quartic models. In Sec. VI and in Part II we show that it also performs consistently well for a wide range of parameters encountered in actual hydrogen-bond systems for which splittings have been measured.

V. TESTS

In this section we test the performance of the rainbow approach for a 2D model systems for which exact instanton solutions for the Euclidean action are known. The 2D model consists of a quartic potential coupled symmetrically to a single harmonic mode, i.e., the 2D quartic model described in Sec. II C [see Eq. (15)]. Since for this model the instanton solution can be found by direct minimization or other technics, we compare here our results with the periodic-orbit solutions $S_I(=2S_E)$ at $T = 0$ reported by Benderskii and Makarov.[21] As we are dealing with a single coupled mode, we omit the subscripts s and i in this section.

For any 2D system of this type, the action S_I is defined by just two parameters, for which we choose $B = \gamma^2/2\omega^2$ and ω (all parameters are dimensionless). Specifically, we explore the behavior of S_I by changing ω while keeping B constant, which implies that the coupling constant $\gamma = \omega\sqrt{2B}$ and the parameter $A = B\omega/2$, defined in Eq. (20), change proportionally to ω. Figures 2 and 3 depict the instanton solutions of Benderskii and Makarov[21] for $B = 0.5$ and $B = 0.8$.

For a given combination (B, ω), the action S_I and the instanton equation are described by Eq. (6), where $V_{ad}(Q) = (1-B)(1-Q^2)^2$; the nonlocal term contains a single symmetric component with $\Lambda = 1 - Q^2$ and $\alpha = B/2\omega$; the characteristic time of motion is $\tau^* = 1/\sqrt{1-B}$. We first summarize the well-known results of the standard treatment in order to demonstrate its failure for the range of parameters of interest. We obtain the "slow-flip" and "fast-flip" solutions by, respectively, replacing the exponential kernel by a delta function and by expanding it, as detailed earlier. Then we solve the corresponding instanton equations for $Q(\tau)$ and evaluate the action (6) for these solutions. This yields (for details see Ref. 6),

$$S_I^{sf} = \frac{3}{2}S_{1D}\sqrt{1-B}\left[\frac{1}{2}\sqrt{1+\Delta m}\left(1-\frac{1}{2\Delta m}\right) + \frac{1}{\sqrt{\Delta m}}\left(1+\frac{1}{4\Delta m}\right)\sinh^{-1}\sqrt{\Delta m}\right],$$
$$S_I^{ff} = 2S_{1D}\left(Q_{0,ff}^3 + \frac{3}{2\sqrt{2}}A\,Q_{0,ff}^2\right), \quad (50)$$

where S_{1D} for the quartic potential is given by Eq. (15) and the parameters are

$$\Delta m = 4\gamma^2/\omega^4; \quad Q_{0,ff} = \sqrt{1+s^2} - s, \quad s = A/(1-B)\sqrt{2}. \quad (51)$$

In Fig. 2, these solutions for $B = 0.5$ are depicted by dashed lines. For this large value of B these two approximations fail unless the frequency of the harmonic mode is either very large

($\omega \geq 3$) or very small ($\omega \ll 1$), leaving a wide range of ω values uncovered. We now show how the new approach bridges this gap.

In terms of our scheme the action $S_{\rm I}$ is given by

$$S_{\rm I} = 2\big(S_{\rm ad} + S_{\rm nl}^{(0)}\big); \quad S_{\rm ad} = (4/3)\sqrt{2(1-B)}, \tag{52}$$

where $S_{\rm nl}^{(0)}$ is given by Eq. (31) which contains a single term with $\alpha = B/2\omega$. Comparison with Benderskii's solution in Fig. 2 shows that Eq. (52) indeed represents the action as a sum of a main term, $2S_{\rm ad} = (8/3)\sqrt{2(1-B)}$, depicted by the dot-dashed line, and a correction, $2S_{\rm nl}^{(0)} > 0$, which is relatively small in the sense that the ratio $(S_{\rm I} - 2S_{\rm ad})/2S_{\rm ad} \leq 20\%$ in the range of interest $\omega \geq \sqrt{1-B}$, covering the region to the right of the short vertical line. This justifies the replacement of $S_{\rm nl}$ by $S_{\rm nl}^{(0)}$ in Sec. II C, whereby the nonlocal action is evaluated with the rainbow solution $Q^{(0)}$. Since there is just a single coupled mode, this solution is obtained from Eq. (6), applying either the AA or the SA to the exponential kernel, which in Eq. (28) leads to $\bar{Q}(\bar{t}) = \bar{Q}^{\rm AA}(\bar{t})$ or $\bar{Q}(\bar{t}) = \bar{Q}^{\rm SA}(\bar{t})$, respectively. From Eq. (20) we obtain for the AA the parameters: $A'' = B'' = 0$, $B' = B$, $\Delta m_s = 4\gamma^2/\omega^4$, and for the SA the parameters: $A'' = A = \gamma^2/4\omega$, $B' = \Delta m = 0$, $B'' = B$. The resulting values $S_{\rm nl}^{\rm AA}$ and $S_{\rm nl}^{\rm SA}$, obtained from Eq. (31), yield upper and lower limits $S_{\rm I}^{\rm AA} = 2[S_{\rm ad} + S_{\rm nl}^{\rm AA}]$ and $S_{\rm I}^{\rm SA} = 2[S_{\rm ad} + S_{\rm nl}^{\rm SA}]$ to the action (52), as depicted by solid lines in Fig. 2. Comparison with the exact result of Benderskii shows that while $S_{\rm I}^{\rm SA}$ provides a satisfactory solution only at very low frequency, the action $S_{\rm I}^{\rm AA}$ performs very well over a wide range of frequencies, down to at least $\omega \sim \sqrt{1-B} = 1/\tau^*$. At still smaller ω, $S_{\rm I}^{\rm AA}$ deviates from the exact solution, more so with larger B, as illustrated in Fig. 3 for $B = 0.3$, 0.5 and 0.8. Note, however, that the stronger the coupling, the smaller will be the range of low frequencies; and the smaller the coupling, the narrower will be the difference between the two limits. The gap between $S_{\rm I}^{\rm AA}$ and $S_{\rm I}^{\rm SA}$ is therefore readily bridged by interpolation, as illustrated in Fig. 3, where the thick lines represent linear interpolation between $S_{\rm I}^{\rm AA}(\omega \simeq \sqrt{1-B})$ and $S_{\rm I}^{\rm SA}(\omega \ll 1)$. Hence this approach can accurately reproduce the instanton action of the 2D quartic model for arbitrary values of the relevant parameters.

VI. APPLICATION TO THE ZERO-LEVEL TUNNELING SPLITTING IN MALONALDEHYDE

Section V shows that the rainbow method yields accurate values for the (dimensionless) instanton action of a 2D model system for a wide range of parameters. To provide a test for real systems of practical interest, we first need to generate the multidimensional Hamiltonian in the form of Eq. (1) from data obtained quantum-chemically. Subsequently, our method will use the resulting Hamiltonian to generate the desired experimental observables, in the present instance zero-point splittings in polyatomic molecules and complexes. In view of the limited experimental data presently available, we will focus on observed splittings assigned to proton and deuteron motion along hydrogen bonds.

A representative list of available examples is presented in Table I, from which it is evident that the magnitude of the splitting shows a strong (exponential) dependence on the adiabatic barrier height, a quantity that is not directly observable but can be calculated with standard quantum-chemical programs. Evidently, such calculations need to be performed at a level that is sufficiently high to yield reliable barrier heights. Any experimental test of the theory presented in this paper thus requires a thorough evaluation of the accuracy of the quantum-chemical input data. An analysis of this kind for the molecular systems listed in Table I will be presented in Part II. Here we limit ourselves to the simplest of them, the molecule malonaldehyde (MA), for which accurate zero-point splittings for both H and D transfer have been measured, namely 21.583 $\rm cm^{-1}$ for MA-d_0 (Ref. 23) and 2.915 $\rm cm^{-1}$ for MA-d_1.[24] In addition, Wang *et al.*[25] reported a full-dimensional *ab initio* potential energy surface, with which they obtained splittings close to the measured values, using a diffusion Monte Carlo method. This massive calculation can serve as a theoretical benchmark.

The parameters needed in our approach we obtain from quantum-chemical data for the equilibrium configuration and the TS in terms of the normal modes of the latter; a detailed description of how the quantum-chemical output is transformed into our input can be found in the Appendix and in Ref. 3. The quantum-chemical data are obtained by standard methods, in this case a hybrid of MC-QCISD/3 and W1BD.[26] Thus the geometries of the stationary points, as well as the Hessians are obtained at the MC-QCISD/3 level. This is a multi-coefficient correlation method which has proved to be cost-effective in several studies of hydrogen abstraction reactions.[27] To obtain accurate reaction energetics (i.e., barrier heights at the TS and along the LRP), single-point W1BD[28] calculations over the previously optimized MC-QCISD/3 geometries were performed. Since the resulting adiabatic barrier height is similar to that obtained by Wang *et al.*,[25] this potential should be adequate for our purpose of testing the rainbow approach. No further efforts were made to "improve" the results by higher-level quantum-chemical calculations.

As pointed out before, the present approach operates with the adiabatic potential along the reaction coordinate. Its width Δx and height U_0, as well as its curvatures in the minimum and at the top, ω_0 and $|\omega^*|$, respectively, are directly obtained from the above calculations at the stationary configurations; they are listed in Table I. For the intermediate region, we either interpolate between the two harmonic curves or we assume a quartic potential; the parameters reported in Tables I–III are based on the quartic potential. Table I compares the relevant quantum-chemical and spectroscopic parameters of MA with those of systems to be analyzed in Part II. Tables II and III list the relevant properties of the coupled modes for MA-d_0 and d_1, respectively. The results show the predominance of symmetric coupling, which amounts to a collective value $B_{\rm s} = 0.70$, which means that it is very strong. By comparison, the value $B_{\rm a} = 0.02$ indicates that antisymmetric coupling is essentially negligible. The symmetric couplings are dominated by a single mode, the O–O hydrogen-bond stretch, indicated in bold in Tables II and III. The antisymmetric couplings are dominated by a deformation mode of the O–H–O group. These dominant modes, as well as all

TABLE II. Parameters of the normal modes of the transition state configuration [symmetric (s) and antysymmetric (a)] contributing to the linear coupling in malonaldehyde-d_0: ω_i, frequencies (in cm^{-1}); Δy_i, displacements defined in Eq. (A9) [in AA $\cdot$ (amu)$^{1/2}$]; B_i, coupling parameters defined in Eq. (9); α_i, kernel coefficients in Eq. (7); ζ_i, zeta-factor defined in Eq. (53) ($\zeta_i > 1$ indicates that the mode is close to the adiabatic limit); R_{1i}, contribution to the mass-renormalization Δm_s or Δm_a defined in Eq. (22) or (35), respectively (in %); R_{2i}, contribution to the (collective) coupling parameters B_s or B_a in Eq. (9) (in %). The dominant hydrogen-bridge symmetric stretching mode is listed in bold.

ω_i	Δy_i	B_i	α_i	ζ_i	R_{1i}	R_{2i}	Symmetry
627	**0.733**	**0.488**	**0.365**	**1.2**	**90.5**	**68.4**	**s**
943	0.192	0.076	0.038	1.9	6.2	10.6	s
1064	0.003	0.000	0.000	2.1	0.0	0.0	s
1361	0.059	0.015	0.005	2.7	0.6	2.1	s
1626	0.006	0.000	0.000	3.2	0.0	0.0	s
1896	0.127	0.134	0.033	3.8	2.7	18.8	s
3109	0.005	0.001	0.000	6.2	0.0	0.1	s
3244	0.000	0.000	0.000	6.4	0.0	0.0	s
569	0.069	0.004	0.003	1.1	71.0	22.9	a
1099	0.005	0.000	0.000	2.2	0.4	0.4	a
1319	0.006	0.000	0.000	2.6	0.5	0.9	a
1492	0.001	0.000	0.000	2.9	0.0	0.0	a
1604	0.043	0.011	0.003	3.1	27.6	70.6	a
3109	0.006	0.001	0.000	6.1	0.5	5.2	a

remaining modes, in both cases fall just into the "fast" category, as indicated by the values of their "zeta-factors,"

$$\zeta_i = \omega_i \tau^* = \omega_i / \sqrt{1 - B}, \tag{53}$$

which are larger than unity. The rainbow solution is thus equivalent to the "slow-flip" solution. Table IV lists the relevant parameters in the final expression (48) for the zero-level splitting, namely the calculated splittings and their counterparts from the model of Sec. III B.

In Table V, our results are compared with experiment and several other calculations. The massive calculation of Wang *et al.*,[25] which is not based on instanton technics, we use as a theoretical benchmark, since their PES, constructed from more than 11 000 calculated points is clearly the most accurate presently available and so is their calculated zero-point level. Their calculated splittings closely match the observed values. In comparison our splittings are too large by 10–15%, although our deuterium isotope effect is accurate, which indicates that the tunneling part is handled well by the method. Thus, in principle, the result could be improved by a slightly higher barrier. However, our barrier height is similar to that of Wang *et al.* A problem that arises in our calculation, and presumably in other instanton calculations as well, is that the tunneling mode is treated as a harmonic oscillator in the equilibrium configuration. This indicates that the rainbow approach will work best for systems with higher barriers, including most of those listed in Table I, for which the anharmonicity will be smaller. With a barrier as low as 4 kcal/mol for malonaldehyde, the mode will be strongly anharmonic, as follows from the observed OH-stretch frequency of 2960 cm^{-1},[24] well below the calculated harmonic frequency of 3371 cm^{-1} obtained in our calculation. A lower frequency would tend to lower the splitting; for MA our

TABLE III. Same as in Table III, for malonaldehyde-d_1.

ω_i	Δy_i	B_i	α_i	ζ_i	R_{1i}	R_{2i}	Symmetry
627	**0.727**	**0.479**	**0.272**	**1.7**	**86.4**	**67.0**	**s**
930	0.230	0.105	0.040	2.4	8.6	14.8	s
1063	0.008	0.000	0.000	2.8	0.0	0.0	s
1340	0.152	0.096	0.025	3.5	3.8	13.4	s
1387	0.080	0.028	0.007	3.6	1.0	4.0	s
1635	0.030	0.006	0.001	4.3	0.1	0.8	s
3109	0.005	0.001	0.000	8.2	0.0	0.1	s
3244	0.000	0.000	0.000	8.5	0.0	0.0	s
568	0.095	0.007	0.004	1.5	96.7	74.6	a
1099	0.003	0.000	0.000	2.9	0.1	0.3	a
1309	0.011	0.000	0.000	3.4	1.3	5.3	a
1487	0.005	0.000	0.000	3.9	0.3	1.4	a
1554	0.010	0.001	0.000	4.0	1.1	6.2	a
3109	0.007	0.001	0.000	8.1	0.5	12.2	a

TABLE IV. Parameters used to calculate the zero-level tunneling splitting ΔE_0 in malonaldehyde (MA-d_0/d_1) from Eqs. (48) and (49). $V_0/\hbar\Omega$ and ω_0 are taken from Table I. The action $\widetilde{S}_{ad}$ is obtained from Eq. (49), where $\widetilde{B}_s$ is from Eq. (37) and S_{1D} from Eq. (15). The nonlocal action $\widetilde{S}^{(0)}_{nl,s}$ is evaluated from Eq. (31) with the rainbow solution of Eq. (28), where Δm_s is the mass-renormalization parameter, given by Eq. (22), and $Q_0 = Q^{(0)}(\tau \to \infty)$ is evaluated from Eq. (27); all evaluated with the rescaled parameters in Eq. (37). Note that all symmetric modes are "fast." The comparison between $\widetilde{S}_{ad}$ and $\widetilde{S}^{(0)}_{nl,s}$ shows that the latter is a relatively small correction, which justifies its evaluation with an approximate instanton solution. The effect of the (weak) antisymmetric coupling is represented by the coefficient C_a defined in Eq. (38); $\Delta S_a = 0$, since the asymmetric modes are also "fast". Also listed is the splitting $\Delta E_0^{(M)}$ evaluated with the model described in Sec. III B. Splittings are in cm^{-1}; all other parameters are dimensionless.

Molecule	$\widetilde{B}_s$	Q_0	Δm_s	C_a	$\widetilde{S}_{ad}$	$\widetilde{S}^{(0)}_{nl,s}$	S_E	ΔE_0	ΔE_0^M
MA-d_0	0.71	1.0	9.67	1.01	1.01	0.26	6.62	25.2	27.4
MA-d_1	0.71	1.0	5.72	1.01	1.01	0.20	8.42	3.4	3.8

TABLE V. Summary of malonaldehyde calculations. ω_0^H is the frequency of the O–H stretching mode in the stable configuration (in cm^{-1}); U_0 the barrier height at the TS (in kcal/mol); $\Delta E_0^{H/D}$, the calculated splittings for MA-d_0/d_1, and KIE = $\Delta E_0^H / \Delta E_0^D$ denotes the isotope effect.

Reference	ω_0^H	U_0	ΔE_0^H	ΔE_0^D	KIE
Observed[a]	2960		**21.583**	**2.915**	**7.40**
Wang *et al.*[b]	3349	4.09	22	3.0	7.3
Mil'nikov[c]	3371	3.61	30.7	4.58	6.7
idem[c,d]	(2845)	(10.0)	57.7	8.63	6.7
idem[c]		3.81	21.2	3.0	7.1
Thompson[e]	2845	10.0	21.8	4.3	5.1
AIM[f]	3548	10.3	19.7	2.6	7.6
Rainbow approx.[g]	3371	4.08	25.2	3.4	7.4
idem (Model)[g]	3371	4.08	27.4	3.8	7.2

[a]References 23 and 24.
[b]Reference 25.
[c]Reference 29.
[d]The same potential was used in Ref. 10 with slightly different results.
[e]Reference 30.
[f]Reference 12(b).
[g]Present work.

estimates show that the splittings based on harmonic frequencies are overestimated by about 10–15%, a correction in the right direction for our results. This problem was avoided by Wang *et al.* by calculating the energy of the zero-point level explicitly for the PES. It is not clear to what extent this problem enters the reported accurate splittings of Mil'nikov *et al.*,[29] who used an instanton procedure. Their calculated deuterium isotope effect is about 5% too low and the barrier they used is about 7% lower than that of Wang *et al.*

An attempt by Thompson *et al.*[30] to construct a PES that adequately reproduces the vibrational force field in the equilibrium configuration gave rise to a barrier height of 10.0 kcal/mol, more than twice the most recent results. Nevertheless, using a semiclassical approach based on Ref. 4, they obtained an accurate value (21.8 cm^{-1}) for the splitting of MA-d_0, although not for that of MA-d_1 (4.3 cm^{-1}). Mil'nikov and Nakamura who used this PES in their invariant instanton method, obtained splittings of 57.7 and 8.6 cm^{-1}, respectively, and concluded that the PES was inadequate.[29] Using different surfaces, these authors and their co-workers later reported values of 30.7 and 4.58 cm^{-1} for a PES with a barrier height of 3.61 kcal/mol, prior to the more accurate values mentioned, reported by Mil'nikov *et al.*[29] mentioned above. In this connection we note that our earlier AIM calculations for MA,[12(b)] based on a potential generated at the HF/6-31G** level, produced a barrier of 10.30 kcal/mol, similar to that of Thompson and yielded comparable splittings. One reason why they were so close to the observed values may be that a high barrier corresponds to a high imaginary frequency, which may reassign a strongly coupled mode from the fast to the slow category, thereby reversing the effect of the coupling from hindering to promoting tunneling. This self-correcting effect reduces the sensitivity of the instanton approach to the precision of the calculated barrier height.

It may be argued that MA is a very simple case, since in the derivation of the rainbow solution, all coupled modes can be treated within the adiabatic approximation. On the other hand, it is one of the toughest tests to meet, both because of the strong coupling and the low barrier height, as seen from Table I. In Part II, we will show that the method works equally well for the remaining molecules and complexes listed in the table. The key reason is that they all belong to the class of strong and dominant symmetric coupling, for which the approach was developed, as indicated by the large values of the collective coupling parameter B. For these systems there are far fewer calculations available and none on the scale of the calculations of Wang *et al.*

VII. DISCUSSION

The method introduced here aims at improving the applicability of instanton methodology to tunneling dynamics in systems with many degrees of freedom. It addresses in particular systems in which the tunneling coordinate is coupled strongly to one or more other (perpendicular) coordinates whose frequency is neither very large nor very small compared to the imaginary frequency of the tunneling coordinate, such that neither the adiabatic (slow-flip) nor the sudden (fast-flip) approximation is adequate for dealing with the coupling. The term "rainbow" expresses the ability of the new method to deal with coupled modes in a wide range of frequencies. Systems considered here are molecules and complexes with a symmetric barrier to proton transfer that is low enough to be penetrated at zero temperature, thus leading to observable level splitting. As an example, the method is applied to proton transfer along hydrogen bonds such as may occur between oxygen and/or nitrogen atoms.

To make effective use of the power of the instanton approach, the method starts from two basic premises. The first is the choice of the configuration of highest symmetry, i.e., the transition state, as the origin of the set of normal coordinates of the system, with couplings to the tunneling coordinate that are kept linear, but subject to higher-order couplings through recalibration of the linear coupling parameters. The instanton methodology then allows integration over the coupled modes, thereby effectively reducing the dynamics to that of a 1D system involving only the tunneling coordinate, the coupling effects being manifested by local and nonlocal terms in the Euclidean action. It favors the development of analytical approximations, which at first sight may look abstruse, but in practice can greatly improve the computational efficiency. This applies in particular if the potential is symmetric, as required for level splitting, because linear coupling implies that only modes that are symmetric or antisymmetric with respect to the symmetry element can affect the splitting. The effect of each coupled mode on the splitting has a specific sign, depending solely on the symmetry and the frequency of the mode as scaled by the overall coupling; its magnitude depends, in addition, on the strength of its specific coupling. The frequency dependence is critical in the case of symmetric coupling, where it determines the sign of the contribution to the splitting. All these effects can be evaluated with good accuracy on the basis of standard electronic-structure and force field data of only the two stationary configurations, implying that corresponding data for the intermediate configurations are not critical but can be deduced from physical arguments based on the symmetry and continuity of the potential.

The second basic premise is that, even in the case of strong coupling, the local part of the Euclidean action dominates the nonlocal part; the latter can therefore be treated as a pertubation that needs to be calculated only approximately. The treatment proceeds with the introduction of the rainbow approximation based on an approximate instanton solution with a conversion property that allows evaluation of the nonlocal term with the exponential kernels intact. This approach offers a satisfactory solution to the critical frequency dependence of the contributions of symmetric modes in systems with strong coupling, as encountered in proton transfer in hydrogen bonds.

The application of the method to 2D model systems for which exact solutions are available shows that the rainbow approximation can provide accurate values for the instanton action of these systems and reduces to the known fast-flip and slow-flip solutions in the appropriate limits. It thus bridges the gap between the adiabatic and the sudden approximations for the parameter range of practical interest. However, the generalization from a 2D to an MD system is not trivial, in particular with respect to the recalibration of the coupling

parameters, mentioned above as a means to simulate higher-order effects of the couplings. As a further test, the method is therefore applied to two isotopomers of malonaldehyde, a widely used benchmark for the calculation of zero-point splittings. The results, based on relatively simple calculations of the equilibrium and transition-state configurations only, show that the method yields reasonably accurate values for the splitting and a very accurate value for its deuterium isotope effect at a fraction of the computation cost of any other competent method presently available. Qualitatively, a good fit to the isotope effect combined with a less accurate fit to the absolute splittings suggests that the barrier is inaccurate, while a good fit to only one of two or three isotopes probed suggests that the tunneling is not well handled. In this respect our calculation compares favorably with several other, more laborious, calculations.

The rainbow approach is a new approximate scheme for direct evaluation of the Euclidean action, which avoids the time-consuming search of the exact instanton trajectory. Due to its computational efficiency, it can be applied to systems of practical interest for which other, more elaborate methods may be at present cost-prohibitive. The procedure to be followed to turn standard quantum-chemical data of the stationary configurations into tunneling splittings is in fact quite simple, as we will demonstrate in more detail in Part II, where we investigate a number of larger molecules and complexes. For the time being, these investigations are limited to systems with hydrogen bonds in which a proton is exchanged between oxygen and/or nitrogen atoms. The van der Waals forces involved are essentially electrostatic and give rise to strong linear coupling of the mobile protons to one or, at most, a few high-frequency skeletal vibrations. To our knowledge no tunneling splittings have been reported for systems in which a neutral hydrogen atom is exchanged between two carbon atoms, one of which is a radical. The van der Waals radii of methyl groups and methylene radicals imply a wide barrier. The kinetic data available for some of these systems, all asymmetric, indicate a strong temperature dependence at low temperatures implying the involvement of low-frequency vibrations.[2] Unfortunately, no actual calculations are available to date.

APPENDIX: GENERATION OF THE HAMILTONIAN

In this part we outline the generation of the Hamiltonian (1) from quantum-chemical data. Tunneling splitting of energy levels occurs when a light particle is exchanged between two equivalent heavier (groups of) particles, as symbolically represented by

$$\mathrm{Y}-\mathrm{X}\cdots\mathrm{Y} \leftrightarrow \mathrm{Y}\cdots\mathrm{X}\cdots\mathrm{Y} \leftrightarrow \mathrm{Y}\cdots\mathrm{X}-\mathrm{Y}, \tag{A1}$$

such that the equivalent structures left and right represent the two equilibrium configurations (EQ), corresponding to energy minima and the central structure is the transition state (TS) corresponding to an energy maximum. As the first step towards calculating the splitting, we describe a system with these three structures in terms of a coordinate system centered at the point of highest symmetry, namely TS, since this will yield the simplest equations. The EQ and TS configurations denote points along the "reaction coordinate" x. Our choice of origen implies that TS is located at $x = 0$; for the location of EQ we use the notation $x_{\mathrm{EQ}} = \pm\Delta x$. The simplest system of this type is a linear triatomic molecule with atomic masses $m_{\mathrm{Y}} = M$, $m_{\mathrm{X}} = m$, $m \ll M$. As in all symmetric linear triatomics, the molecular vibrations will be governed by three normal coordinates, a symmetric stretching mode to be denoted by y, an antisymmetric stretching mode denoted by x and a bending mode, which we will ignore since it is not displaced during the tunneling. However, since the origen TS is an energy *maximum*, the motion along x will be highly anharmonic; the negative curvature of the potential implies that we can characterize this motion near $x = 0$ by an imaginary harmonic frequency $i\omega^*$. This is the motion that gives rise to the tunneling splitting. Because of its anharmonicity, it is coupled in lowest order to y. We use the notation (x, y) for the (mass-weighted) normal modes, and (Q, q) for their dimensionless counterparts, as in the main text.

As a preliminary to the MD Hamiltonian in Eq. (1), we derive the vibrational Hamiltonian of the collinear system (A1). Excluding the center of mass, and assuming harmonic forces with force constants $k_{\mathrm{X\text{-}Y}}$ and $k_{\mathrm{Y\text{-}Y}}$, this Hamiltonian in dimensionless form is given by

$$H = \frac{1}{2}\dot{Q}^2 + \frac{1}{2}\dot{q}^2 + (|Q| - 1)^2 + \frac{1}{2}\omega^2 q^2 - \gamma(|Q| - 1)q. \tag{A2}$$

The dimensionless normal coordinates (Q, q) are related to the mass-weighted normal coordinates (x, y) via $Q = x/\Delta x$ and $q = y/\Delta x$. To define the coordinates we introduce Cartesian coordinates d_2 for X and $d_{1,3}$ for Y, so that $x = \frac{1}{2}\sqrt{\mu_0}\,[(d_1 - d_3) - d_2]$ and $y = \sqrt{\mu}\,[(d_3 - d_1) - (d_3 - d_1)_{\mathrm{EQ}}]$ with reduced masses $\mu_0 = 2Mm/(2M + m)$ and $\mu = M/2$, and frequencies $\boldsymbol{\omega}_0 = \sqrt{k_{\mathrm{X-Y}}/\mu_0}$ and $\boldsymbol{\omega}_{13} = \sqrt{k_{\mathrm{Y-Y}}/\mu}$, respectively. The potential along the reaction coordinate equals $V(x) = \frac{1}{2}\boldsymbol{\omega}_0^2(|x| - \Delta x)^2$ with $V(0) \equiv V_0$ and $\Delta x = \frac{1}{2}\sqrt{\mu_0}\,[(d_3 - d_1)_{\mathrm{EQ}} - 2(d_2 - d_1)_{\mathrm{EQ}}]$. In Eq. (A2) energy is scaled by V_0; time and frequency are measured in units of the scaling frequency $\boldsymbol{\Omega}$, defined as $V_0 = \boldsymbol{\Omega}^2\Delta x^2$. The tunneling motion is coupled to the harmonic oscillator q, which describes the relative motion of the Y atoms with frequency $\omega = \sqrt{(\boldsymbol{\omega}_{13}/\boldsymbol{\Omega})^2 + \gamma^2/2}$, $\gamma = \sqrt{\mu_0/\mu}$ being the coupling constant. For clarity we use, in this Appendix only, bold/ordinary symbols ω and Ω for dimensional/dimensionless frequencies, respectively.

The double-minimum potential in Eq. (A2) is formed by crossing parabolas and thus has a cusp at $Q = 0$; it is usually replaced by a smooth potential, for which the quartic potential $V_{1\mathrm{D}}(Q) = (1 - Q^2)^2$ is a standard choice. Equation (A2) then takes the form

$$H = \frac{1}{2}\dot{Q}^2 + \frac{1}{2}\dot{q}^2 + (Q^2 - 1)^2 + \frac{1}{2}\omega^2 q^2 - \gamma(Q^2 - 1)q. \tag{A3}$$

The potentials (A2) and (A3) are defined so that $q = 0$ at EQ; we redefine them so that $q = 0$ at TS and $q = \pm\Delta q = \pm\gamma/\omega^2$ at EQ, after which the above potential reads

$$V(Q, q) = V_{1\mathrm{D}}(Q) + \frac{1}{2}\omega^2(q^2 - \Delta q^2) - \gamma Q^2(q - \Delta q). \tag{A4}$$

The 1D potential along the reaction coordinate we actually use is the adiabatic potential $V_{\rm ad}(Q)$, which is defined from Eq. (A4) along the trajectory $\partial V(Q,q)/\partial q = 0$; then Eq. (A4) assumes the familiar form

$$V(Q,q) = V_{\rm ad}(Q) + \frac{1}{2}\omega^2\left(q - \frac{\gamma}{\omega^2}Q^2\right)^2. \tag{A5}$$

In Eqs. (A2) and (A3), the double-minimum potential along the reaction coordinate corresponds to $V(Q,q)$ evaluated at $q = \Delta q$, i.e., with the heavy atoms "frozen" in their equilibrium position; we call this potential "crude-adiabatic". With this choice of $V_{\rm 1D}(Q)$, the adiabatic potential can be formulated as

$$V_{\rm ad}(Q) = (1-B)V_{\rm 1D}(Q); \quad B = \gamma^2/2\omega^2 < 1, \tag{A6}$$

i.e., $V_{\rm 1D}(Q)$ and $V_{\rm ad}(Q)$ are of the same shape, with minima equal to 0 at $|Q| = 1$ and maxima equal to 1 and $1 - B$ at $Q = 0$. The coupling parameter B thus measures the reduction of the barrier height induced by the symmetric Y···Y-stretching vibration.

The calculations operate with potentials in the form of Eqs. (A5) and (A6); setting the minimum of $V_{\rm ad}(Q)$ equal to zero, we obtain for the potential (A5) about the minima $|Q| = 1$ and the transition state $Q = 0$,

$$\begin{aligned} V_{\rm EQ} &= \frac{1}{2}\omega_0^2(|Q|-1)^2 + \frac{1}{2}\omega^2(q-\Delta q)^2, \\ V_{\rm TS} &= (1-B) - \frac{1}{2}|\omega^*|^2Q^2 + \frac{1}{2}\omega^2q^2, \end{aligned} \tag{A7}$$

ω_0 and $i\omega^*$ being the real and imaginary frequencies in the minima and at the maximum of $V_{\rm ad}(Q)$, respectively. This presentation shows that Q and q are the normal modes of the TS-configuration, Q being the mode with imaginary frequency. It also shows that the normal mode q, which represents the skeletal motion, does not change its form and frequency between the stationary configurations, but undergoes only a displacement Δq.

Equations (A4)–(A7) can be generalized to the MD case where Y represents a structure composed of many atoms and subject to many vibrations. We summarize here the main steps; details can be found in Ref. 3. We generate the Hamiltonian in the form of Eq. (1) using the set of (mass-weighted) normal modes $(x, \{y_i\})$ of the TS configuration centered at $(x = 0, \{y_i\} = 0)$. The mode x with imaginary frequency is again the "reaction coordinate," to which the remaining skeletal modes $\{y_i\}$ are linearly coupled. Only modes that are displaced between the stationary configurations contribute to this coupling. These modes are separated into symmetric $(i = {\rm s})$ and antisymmetric $(i = {\rm a})$ groups, depending on their symmetry with respect to reflection in the dividing plane $x = 0$. Their displacements at the minima are $\pm\Delta x; \pm\{\Delta y_{i={\rm s}}\}$ for the antisymmetric modes and $\{\Delta y_{i={\rm s}}\}$ for the symmetric modes. The crude-adiabatic potential $V_{\rm 1D}(x)$, which by definition corresponds to the atoms in Y frozen in their equilibrium positions, is evaluated along the LRP. As before, the height V_0 and (mass-weighted) halfwidth Δx of this potential are the scaling parameters for energies and coordinates, respectively. Frequencies and time are scaled by the scaling frequency $\boldsymbol{\Omega}$, defined as $\boldsymbol{\Omega}^2\Delta x^2 = V_0$. The linear coupling constants γ_i are related to the (dimensionless) displacements and frequencies as

$$\gamma_i = \omega_i^2\Delta q_i; \quad \Delta q_i = \Delta y_i/\Delta x. \tag{A8}$$

We use these relations in reverse, i.e., we evaluate the coupling constants from the frequencies and displacements, which we calculate from the corresponding atomic displacements, as follows:

$$\Delta x = \sum_{n=1}^{N}\sqrt{M_n}\,r_n\hat{L}_{n,1}, \quad \Delta y_i = \sum_{n=1}^{N}\sqrt{M_n}\,r_n\hat{L}_{n,i}. \tag{A9}$$

Here $\sqrt{M_n}\,r_n$ are the mass-weighted atomic displacements between the TS and EQ; $\hat{L}$ is the $3N \times (3N-6)$ matrix that relates the normal modes of the TS configuration to the Cartesian coordinates of a nonlinear system with N atoms. Finally, introducing the dimensionless coordinates as $Q = x/\Delta x$ and $q_i = y_i/\Delta x$, scaling energy by V_0, and time and frequencies by $\boldsymbol{\Omega}$, we arrive at the potential in the form of Eq. (A5), generalized to the MD case,

$$\begin{aligned} V(Q,\{q\}) = V_{\rm ad}(Q) &+ \frac{1}{2}\sum_{i={\rm s}}\omega_i^2\left(q_i - \frac{\gamma_i}{\omega_i^2}Q^2\right)^2 \\ &+ \frac{1}{2}\sum_{i={\rm a}}\omega_i^2\left(q_i - \frac{\gamma_i}{\omega_i^2}Q\right)^2, \end{aligned} \tag{A10}$$

where the adiabatic potential is defined by Eq. (2).

Analogous to Eq. (A7), the potential $V(Q,\{q\})$ about EQ has the form

$$\begin{aligned} V(Q,\{q\})_{\rm EQ} \simeq \frac{1}{2}\omega_0^2(Q\pm 1)^2 &+ \frac{1}{2}\sum_{i={\rm a}}\omega_i^2(q_i \pm \Delta q_i)^2 \\ &+ \frac{1}{2}\sum_{i={\rm s}}\omega_i^2(q_i - \Delta q_i)^2, \end{aligned} \tag{A11}$$

where ω_0 is an effective harmonic frequency associated with the reaction coordinate in EQ. This frequency is evaluated from the relation between the two sets of normal modes $\{z\}$ and $(x, \{y_i\})$ of the equilibrium and TS configurations, respectively, given by a unitary matrix $\mathbf{G}$;[3] thus

$$x = \sum_j G_{0j}z_j, \quad \sum_j G_{0j}^2 = 1, \tag{A12}$$

so that

$$\boldsymbol{\omega}_0^2 = \sum_j G_{0j}^2\boldsymbol{\omega}_{0j}^2, \tag{A13}$$

where $\boldsymbol{\omega}_{0j}$ are the frequencies of the normal modes $\{z\}$ in EQ; the frequency ω_0 in (A11) is the dimensionless counterpart $\omega_0 = \boldsymbol{\omega}_0/\boldsymbol{\Omega}$. Note that the displacements (A9) and the transformations (A12) are carried out in such a way that the Eckart conditions are obeyed. This is necessary in order to conserve the linear and angular momenta and thus prevent mixing of the vibrations with translations or rotations. Details can be found in Ref. 3.

Similar to the collinear model, the normal modes in Eq. (A10) and in Eq. (1), which describe the skeletal vibrations, do not change their form and frequency between the stationary configurations, as easily seen from Eq. (A10). To account for such changes, as well as for frequency shifts and anharmonicities, higher-order coupling terms would be needed, but these are not explicitly included in our approach, since they would prevent the integration over harmonic oscillators required for instanton applications. To account for the effects of such terms, we recalibrate the linear coupling constants γ_i in Eq. (1) so as to match the adiabatic barrier height $(1 - B)V_0$ (in dimensional units), obtained from Eq. (A6), to the barrier height U_0 obtained quantum-chemically for the *real* PES (see Table I). This recalibration takes the form

$$\gamma_i \rightarrow \gamma_i\sqrt{R}; \quad R = (V_0 - U_0)/E_\mathrm{r}; \quad E_\mathrm{r} = \frac{1}{2}\sum_{i=\mathrm{a,s}} \boldsymbol{\omega}_i^2 \Delta y_i^2, \tag{A14}$$

where E_r represents the "reorganization energy".

For practical applications we also need to specify the shape of the adiabatic potential $V_\mathrm{ad}(Q)$ along the reaction coordinate *between* the stationary points. In this range we either interpolate between the harmonic curves given by the calculated curvatures or we assume an analytical function. The simplest of these, i.e., the one with the lowest powers of Q, is the quartic form $(1 - Q^2)^2$, which is favored in the present paper, since it has proved to be well suited to proton-transfer processes. For a given $V_\mathrm{ad}(Q)$, we can also specify the shape of the crude-adiabatic potential $V_\mathrm{1D}(Q)$ under certain conditions. Namely, if $V_\mathrm{ad}(Q)$ is of the general form $V_\mathrm{ad}(Q) = (1 - B)F(|Q|)$, where $F(\pm 1) = 0$; $F(0) = 1$, and B is defined, analogously to Eq. (A6) as

$$B_\mathrm{a,s} = \sum_{i=\mathrm{a,s}} \gamma_i^2/2\omega_i^2, \tag{A15}$$

the crude-adiabatic potential is $V_\mathrm{1D}(Q) = F(|Q|)$, i.e., the two potentials are of the same shape. This relation is exact for crossing parabolas but only approximate for the quartic potential; however, if $V_\mathrm{ad}(Q) = (1 - B)(1 - Q^2)^2$, then $V_\mathrm{1D}(Q)$ is very well approximated by $(1 - Q^2)^2$ in the case where $B_\mathrm{a} \ll B_\mathrm{s}$, which applies to hydrogen bonds. The relation between the two potentials is therefore as the one given by Eqs. (8) and (9). Note that a meaningful problem requires that $B < 1$, i.e., $E_\mathrm{r} < V_0$, which is well met since the "reaction coordinate" is the mode most displaced in the tunneling process.

If, for very large systems, evaluation of the barrier height V_0 along the LRP is not practical, one can instead use the approximation $V_0 \simeq V_{0,L} = U_0 + E_\mathrm{r}$, which sets $R = 1$ in Eq. (A14). In applications, we use, whenever practical, the rescaled values of the γ_i, but retain the notation of the main text for convenience.

In conclusion we note that all input parameters needed for practical applications of the approach are generated by the DOIT code,[3] which reads directly from standard output of electronic-structure and force-field calculations for the stationary configurations.

[1] S. Coleman, in *The Whys of Subnuclear Physics*, edited by A. Zichichi (Plenum, New York, 1979), p. 805; A. I. Vainshtein, V. I. Zakharov, V. A. Novikov, and M. A. Shifman, "ABC of instantons," Sov. Phys. Usp. **25**, 195 (1982); V. A. Benderskii, D. E. Makarov, and C. H. Wight, Adv. Chem. Phys. **88**, 1 (1994).

[2] See for example, Z. Smedarchina, W. Siebrand, A. Fernández-Ramos, and Q. Cui, J. Am. Chem. Soc. **125**, 243 (2003); W. Siebrand, Z. Smedarchina, J. Phys. Chem. B **115**, 7679 (2011).

[3] W. Siebrand, Z. Smedarchina, M. Z. Zgierski, and A. Fernández-Ramos, Int. Rev. Phys. Chem. **18**, 5 (1999); Z. Smedarchina, A. Fernández-Ramos, and W. Siebrand, J. Comput. Chem. **22**, 787 (2001).

[4] N. Makri and W. H. Miller, J. Chem. Phys. **91**, 4026 (1989).

[5] D. G. Truhlar and A. Kupperman, J. Am. Chem. Soc. **93**, 1840 (1971).

[6] V. A. Benderskii, V. I. Goldanskii, and D. E. Makarov, Chem. Phys. Lett. **171**, 91 (1990); Chem. Phys. **154**, 407 (1991).

[7] C. S. Tautermann, A. F. Voegele, T. Loerting, and K. R. Liedl, J. Chem. Phys. **117**, 1962 (2002); **117**, 1967 (2002).

[8] R. Meana-Pañeda, D. G. Truhlar, and A. Fernández-Ramos, J. Chem. Theory Comput. **6**, 6 (2010).

[9] G. V. Mil'nikov and H. Nakamura, J. Chem. Phys. **115**, 6881 (2001); **122**, 124311 (2005).

[10] J. O. Richardson, S. C. Althorpe, and D. J. Wales, J. Chem. Phys. **134**, 054109 (2011); **135**, 124109 (2011).

[11] J. B. Rommel and J. Kästner, J. Chem. Phys. **134**, 18407 (2011).

[12] (a) Z. Smedarchina, W. Siebrand, M. Z. Zgierski, and F. Zerbetto, J. Chem. Phys. **102**, 7024 (1995); (b) Z. Smedarchina, W. Siebrand, and M. Z. Zgierski, J. Chem. Phys. **103**, 5326 (1995).

[13] Z. Smedarchina, W. Siebrand, and M. Z. Zgierski, J. Chem. Phys. **104**, 1203 (1996); Z. Smedarchina, A. Fernández-Ramos, and M. A. Rios, J. Chem. Phys. **106**, 3956 (1997); A. Fernández-Ramos, Z. Smedarchina, and W. Siebrand, J. Chem. Phys. **109**, 1004 (1998); A. Fernández-Ramos, Z. Smedarchina, and F. Pichierri, Chem. Phys. Lett. **343**, 627 (2001); Z. Smedarchina, W. Siebrand, A. Fernández-Ramos, and E. Martínez-Núñez, Chem. Phys. Lett. **386**, 396 (2004); J. R. Roscioli, D. W. Pratt, Z. Smedarchina, W. Siebrand, and A. Fernández-Ramos, J. Chem. Phys. **120**, 11351 (2004); Z. Smedarchina, A. Fernández-Ramos, and W. Siebrand, J. Chem. Phys. **122**, 134309 (2005).

[14] Z. Smedarchina, W. Siebrand, and A. Fernández-Ramos, Chem. Phys. Lett. **395**, 339 (2004).

[15] F. Madeja and M. Havenith, J. Chem. Phys. **117**, 7162 (2002).

[16] C. S. Tautermann, A. F. Voegele, and K. R. Liedl, J. Chem. Phys. **120**, 631 (2004).

[17] M. Ortlieb and M. Havenith, J. Phys. Chem. A **111**, 7355 (2007).

[18] V. A. Benderskii, E. V. Vetoshkin, S. Yu. Grebenshchikov, L. von Laue, and H. P. Trommsdorff, Chem. Phys. **219**, 119 (1997).

[19] J. P. Sethna, Phys. Rev. B **24**, 698 (1981); **25**, 5050 (1982).

[20] See for example the review, A. O. Caldeira and A. J. Leggett, Ann. Phys. **149**, 374 (1983).

[21] V. A. Benderskii and D. E. Makarov, Chem. Phys. **170**, 275 (1993).

[22] V. A. Benderskii, D. E. Makarov, and D. I. Pastur, Chem. Phys. **161**, 51 (1992).

[23] D. W. Firth, K. Beyer, M. A. Dvorak, S. W. Reeve, A. Q. Gushov, and K. Leopold, J. Chem. Phys. **94**, 1812 (1991); T. Baba, T. Tanaka, I. Morino, K. M. T. Yamada, and K. Tanaka, J. Chem. Phys. **110**, 4131 (1999).

[24] S. L. Baughcum, Z. Smith, E. B. Wilson, and R. W. Duerst, J. Am. Chem. Soc. **106**, 2260 (1984).

[25] Y. Wang, B. J. Braams, J. M. Bowman, S. Karter, and D. P. Tew, J. Chem. Phys. **128**, 224314 (2008).

[26] B. J. Lynch and D. G. Truhlar, J. Phys. Chem. A **107**, 3898 (2003).

[27] J. Zheng, Y. Zhao, and D. G. Truhlar, J. Phys. Chem. A **111**, 4632 (2007).

[28] E. C. Barnes, G. A. Petersson, J. A. Montgomery, M. J. Frisch, and J. M. L. Martin, J. Chem. Theory Comput. **5**, 2687 (2009).

[29] G. V. Mil'nikov, K. Yagi, T. Taketsugu, H. Nakamura, and K. Hirao, J. Chem. Phys. **119**, 10 (2003); **120**, 5036 (2004).

[30] Y. Guo, T. D. Sewell, and D. L. Thompson, Chem. Phys. Lett. **224**, 470 (1994); T. D. Sewell, Y. Guo, and D. L. Thompson, J. Chem. Phys. **103**, 8557 (1995).

[31] A. Vdovin, J. Waluk, B. Dick, and A. Slenczka, ChemPhysChem **10**, 761 (2009).

[32] K. Remmers, W. L. Meerts, and I. Ozier, J. Chem. Phys. **112**, 10890 (2000).

[33] D. R. Borst, J. R. Roscoli, D. W. Pratt, G. M. Florio, T. S. Zwier, A. Müller, and S. Leutwyler, Chem. Phys. **283**, 341 (2002).